Evolution of Structure-guided Drug Design Strategies Targeting Mutations in Codon 12 of KRAS

Journal:	*RSC Medicinal Chemistry*
Manuscript ID	MD-REV-02-2025-000169.R2
Article Type:	Review Article
Date Submitted by the Author:	15-May-2025
Complete List of Authors:	Dorandish, Sadaf; Wayne State University, Department of Pharmaceutical Sciences Bhayekar, Komal; Wayne State University, Department of Pharmaceutical Sciences Singh, Anuradha; Indian Institute of Technology (Indian School of Mines), Department of Chemistry and Chemical Biology Kushwaha, Narva Deshwar; Wayne State University, Department of Pharmaceutical Sciences Malin, Evan; Wayne State University, Department of Pharmaceutical Sciences Serafimovski, Sara; Wayne State University, Department of Pharmaceutical Sciences Kelm, Jeremy M.; Wayne State University, Department of Pharmaceutical Sciences Gavande, Navnath; Wayne State University, Department of Pharmaceutical Sciences; Wayne State University School of Medicine Lakkaniga, Naga Rajiv; Indian Institute of Technology (Indian School of Mines) Dhanbad, Department of Chemistry and Chemical Biology

Evolution of Structure-guided Drug Design Strategies Targeting Mutations in Codon 12 of KRAS.

Sadaf Dorandish[1,#], Komal Bhayekar[1,#], Anuradha Singh[2,#], Narva Deshwar Kushwaha[1], Evan Malin[1], Sara Serafimovski[1], Jeremy M. Kelm[1], Navnath S. Gavande[1,3,*] and Naga Rajiv Lakkaniga[2,*]

[1]Department of Pharmaceutical Sciences, Eugene Applebaum College of Pharmacy and Health Sciences, Wayne State University, Detroit, MI 48201.

[2]Department of Chemistry and Chemical Biology, Indian Institute of Technology (Indian School of Mines), Dhanbad, India 826004.

[3]Molecular Therapeutics Program, Barbara Ann Karmanos Cancer Institute, Wayne State University School of Medicine, Detroit, MI 48201.

[#]These authors contributed equally to this work.

***Corresponding Authors**

Navnath S. Gavande (NSG), Email: ngavande@wayne.edu; Phone: +1-(313)-577-1523; Fax: +1-(313)-577-2033; ORCID ID: orcid.org/0000-0002-2413-0235

Naga Rajiv Lakkaniga (NRL), Email: nagarajiv@iitism.ac.in; Phone: +91-326-223-5550; ORCID ID: orcid.org/0000-0001-8370-2224

Keywords: KRAS (Kirsten rat sarcoma viral oncogene), KRAS mutations, Small molecule inhibitors, Structure-guided drug design, cancer therapy.

Running title: Targeting Mutations in Codon 12 of KRAS.

ABSTRACT

KRAS mutations at codon 12 are among the most frequent driver mutations oncogenic alterations in various cancers and associated with aggressive disease and poor clinical outcomes. Historically, KRAS had been a very difficult target due to its strong binding to GDP/GTP and the lack of available druggable binding pockets. Considerable advances have been achieved in generating direct small-molecule inhibitors selectively targeting KRAS G12 mutations. This review discusses the development of approaches to design inhibitors that bind directly to KRAS, starting from the pioneering work of the Shokat group. This review details significant milestones of KRAS-targeted drug discovery and the current impediments in this field. The identification of covalent inhibitors of the KRAS G12C and more recently a direct inhibitor of K-Ras G12C in a GTP-bound state exemplifies the promise of this approach. Structure-guided drug design improved the basis for understanding the mutations in KRAS, notably at codon 12, and the idea has potential for gene therapy. Focusing exclusively on direct and indirect KRAS inhibitors, this review highlights the evolving strategies transforming KRAS from an elusive target to a tractable therapeutic opportunity, offering new hope for patients with KRAS-driven cancers.

1. Introduction

KRAS (Kirsten rat sarcoma viral oncogene) is a gene within the RAS family of oncogenes, encoding proteins involved in cell signaling pathways that regulate growth and differentiation. It is evolutionarily conserved and primarily expressed as the KRAS-4B isoform, which plays a critical role in cancer development.[1] KRAS mutations are prominent in several cancers, including, pancreatic cancer,[2,3] non-small cell lung cancer,[4,5] and colorectal cancer,[5,6] making it an essential oncogenic driver.[7] These mutations predominantly occur at codons 12, 13, and 61[8], leading to constitutive activation of KRAS, and persistent stimulation of downstream MAPK[9] and PI3K[10,11] signaling pathways.

Among the major cancer types affected by KRAS mutations, NSCLC shows distinct mutation patterns. KRAS mutations in NSCLC account to about 20-25% of lung adenocarcinomas in western countries and 10-15% in Asian counterparts.[12–16] In NSCLC, G12C mutation occurs in about ~40%, G12V mutation in about 19%, and G12D mutation in about 15% (**Figure 1**) of patients with KRAS G12 mutations.[15,16] While NSCLC shows the prominence of G12C mutations, colorectal cancer (CRC) presents a different mutation profile. KRAS mutations are identified in approximately 40% of CRC patients. As of 2018, colorectal cancer ranks third in global cancer incidence and second in cancer-related mortality.[17] These mutations primarily occur at codons 12, 13, and 61, with G12D (42%) being the most prevalent, followed by G12V (22%) and G12A (7%) (**Figure 1**).[18,19] KRAS mutations in CRC are associated with resistance to EGFR inhibitors such as cetuximab and panitumumab.[18,20] Among all KRAS-mutated cancers, pancreatic cancer shows the highest mutation frequency. Pancreatic ductal adenocarcinoma (PDAC) shows the highest KRAS mutation rate, occurring in up to 95% of cases.[2] PDAC constitutes around 90% of all

pancreatic tumors. The G12D mutation is the most common alteration (51%), while G12V and G12R contribute to 30% and 12% of cases, respectively (**Figure 1**).[20,21]

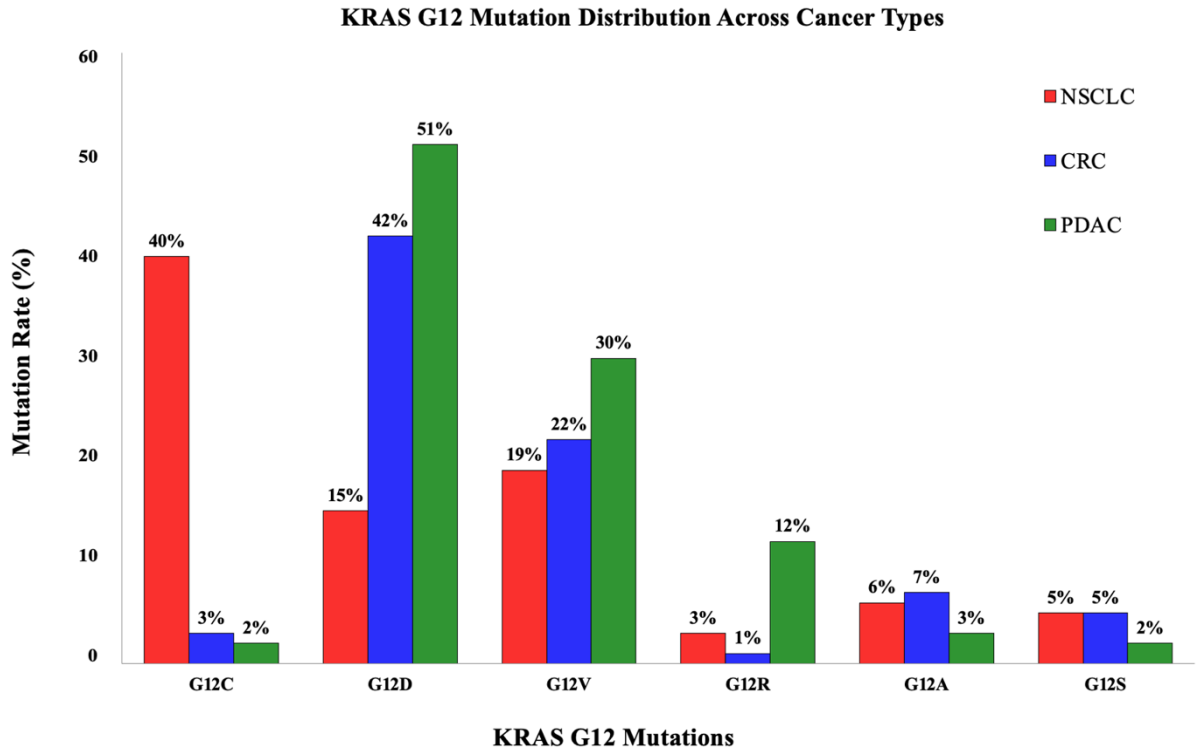

Figure 1. KRAS G12 Mutation Distribution in Major Cancer Types. The bar graph illustrates the distribution of KRAS G12 mutations (G12C, G12D, G12V, G12R, G12A, G12S) across NSCLC, CRC, and PDAC. Each cancer type exhibits distinct mutational patterns, with G12C dominating NSCLC, G12D in CRC and PDAC, and other mutations showing cancer-specific preferences. Percentages are approximate with a margin of error of ±5%.

Understanding the molecular mechanisms underlying KRAS function is critical for the development of effective inhibitors. KRAS operates as a molecular switch,[22] with the nucleotide-binding pocket region being critical for interacting with downstream effectors. This control of KRAS activation occurs by either binding with GTP (active/ON state) or GDP (inactive/OFF state).[10] KRAS exhibits a high affinity for GTP, rendering the development of competitive inhibitors particularly challenging due to the picomolar binding strength and the high intracellular concentration of GTP. Furthermore, the absence of well-defined druggable binding pockets on the KRAS surface contributed to the historical perception of KRAS as "undruggable." For over three

decades, efforts to develop direct KRAS inhibitors yielded limited success. Consequently, alternative strategies targeting the KRAS signaling axis were explored to achieve indirect inhibition. These included inhibitors of post-translational modifications essential for KRAS membrane localization and function, such as farnesyltransferase inhibitors (FTIs), Ras-converting enzyme 1 (Rce1) inhibitors, isoprenylcysteine carboxyl methyltransferase (ICMT) inhibitors, and PDEδ inhibitors, which disrupt KRAS trafficking by impairing its interaction with chaperones. Additionally, compounds targeting the interaction between RAS and its guanine nucleotide exchange factor SOS emerged as another strategy to modulate KRAS activation indirectly.

In this review, we present the evolution of structure-based drug design strategies targeting KRAS G12 mutations, notably G12C and G12D. The following section offers a concise overview of KRAS structural biology, highlighting key functional domains and their relevance to signal transduction and effector engagement. The subsequent section details the evolution of direct KRAS inhibitors, beginning with the seminal discovery from the Shokat lab that identified a cryptic allosteric pocket in KRAS G12C, enabling the development of covalent inhibitors. This breakthrough redefined the druggability of KRAS and catalyzed rapid progress in the development of mutation-specific inhibitors. Further, we present the design strategies and medicinal chemistry behind the identification of various key inhibitors targeting KRAS G12 mutations. Together, these insights into KRAS structure and inhibitor design strategies provide a foundation for guiding design of future therapeutic strategies against KRAS-driven cancers.

2. Structural Biology and Biochemistry of KRAS

KRAS is the most extensively characterized oncogenic isoform of the RAS family, playing a pivotal role in regulating cellular signaling pathways,[23,24] including, cell differentiation,[25,26] growth, and survival. KRAS transmits signals from cell surface receptors to intracellular targets, and toggles between ON and OFF states. Despite distinct differences among the RAS isoforms, namely, KRAS, HRAS (Harvey rat sarcoma virus oncogene), and NRAS (Neuroblastoma rat sarcoma virus oncogene), they all function as small GTP-binding proteins that serve as molecular switches, translating extracellular cues into the activation of downstream signaling pathways.[27]

2.1 KRAS structure

There are two isoforms of KRAS: KRAS 4A (188 amino acids) and KRAS 4B (189 amino acids), both with an approximate molecular weight of 21 kDa. These isoforms consist of four key domains: the G-domain, the C-terminal domain, switch-I, and switch-II.[28,29] Despite their structural similarities, the isoforms differ significantly in features critical for membrane localization and interactions, which in turn affect their signaling function.[30]

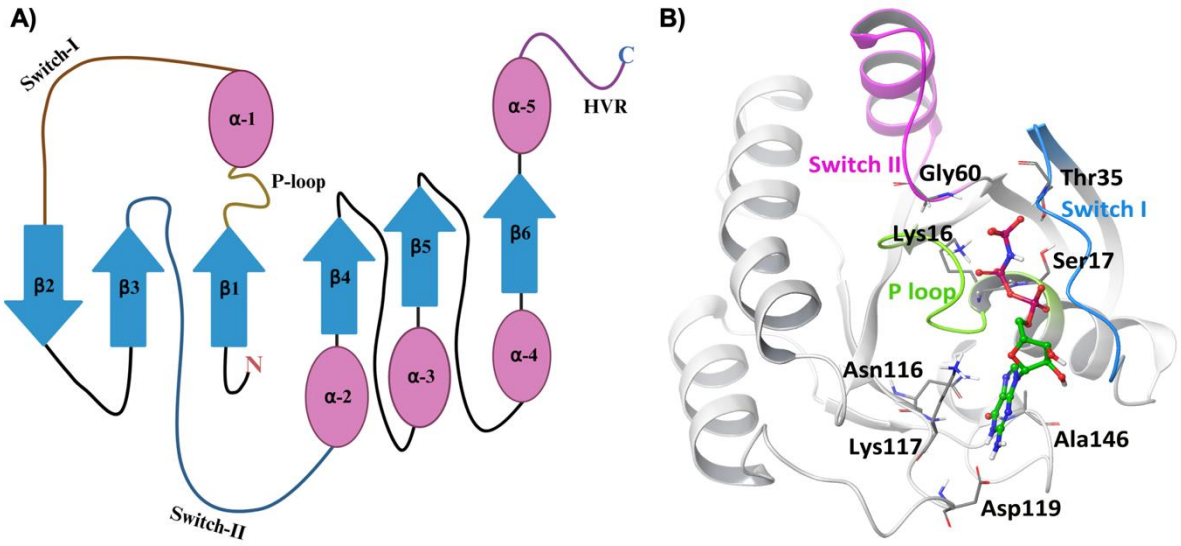

Figure 2: KRAS structural organization and nucleotide-dependent conformational states. A) Overview of KRAS protein structure showing the G-domain, C-terminal domain, switch-I, and switch-II regions. The protein comprises six β-strands forming the core and five α-helices surrounding them. HVR: hypervariable region. B) Detailed view of KRAS active conformation highlighting key conserved residues. Gly60 and Thr35 are linked by hydrogen bonds to the GppNHp molecule (a nonhydrolyzable GTP analog). The Switch II region (magenta), Switch I (blue), and P-loop (green) are shown. This structural arrangement is crucial for KRAS function and regulation.

The KRAS protein consists of two main structural components: the G-domain (residues 1-166), which mediates guanine nucleotide binding and hydrolysis, and the C-terminal hypervariable region (residues 167-189), which undergoes post-translational modifications necessary for membrane association.[31] Within the G-domain, two distinct lobes are recognized: the effector lobe (residues 1-86) and the allosteric lobe (residues 87-166). The effector lobe is highly conserved across RAS isoforms and plays a critical role in interactions with downstream effectors and regulatory proteins. The allosteric lobe, which exhibits greater sequence variability, is involved in modulating conformational states and facilitating membrane interactions.

Three key functional motifs reside within the effector lobe: the phosphate-binding loop (P-loop), Switch I, and Switch II. The P-loop, located between residues 10 and 14 (occasionally extended to 17), interacts with the phosphate groups of GDP and GTP and is a frequent site of oncogenic mutations, particularly at glycine 12. Switch I, spanning residues 30 to 40, is conformationally dynamic and critical for effector engagement, including interactions with RAF, PI3K, and RALGDS. Its structural configuration is highly dependent on the nucleotide-bound state of KRAS. Switch II, comprising residues 58 to 76, contributes to the regulation of GTP hydrolysis and is involved in binding to GTPase-activating proteins. This region is also a key binding site for several small-molecule inhibitors targeting KRAS G12C, particularly in the GDP-bound inactive conformation.

Located between Switch I and Switch II is a shallow cleft termed the Switch I/II interface. This region forms a druggable pocket approximately 5 Å deep and 7 Å wide and is formed by contributions from residues such as K5, R41, D54, T74 (from the α2 helix), and L56 (from the adjacent β-sheet). The interface has become a valuable target in the design of non-covalent KRAS inhibitors, especially for mutants that lack a reactive cysteine residue. Compounds such as BI-2852 and DCAI exploit this site to interfere with KRAS-SOS1 interactions and effector engagement. Overall, the Switch I, Switch II, and their interface are structurally and functionally integral to KRAS signaling and represent key regions for therapeutic intervention in RAS-driven cancers.

When GTP is bound to KRAS with the aid of effector proteins, switches I and II undergo conformational changes and cause GDP-GTP exchange.[32] The nucleotide-binding pocket plays a critical role for interacting with potential downstream effectors and regulates KRAS activation by binding with GTP (active state) or GDP (inactive state).[10] Catalytic residues mediate the hydrolysis of GTP to GDP, enabling KRAS to inactivate itself through its intrinsic GTPase activity. The hypervariable region (HVR) of the C-terminal comprises residues from 167-188, including the CAAX motif that directs three PTMs, which are farnesylation, CAAX proteolysis, and carboxymethylation of C-terminal prenylcysteine.[33] The HVR determines KRAS localization and anchoring at the particular site on the plasma membrane and plays a key role in regulating its biological activities.[34] KRAS4A contains palmitoylated cysteines, whereas KRAS4B features a polylysine sequence preceding the CAAX motif. These features enable both isoforms of KRAS to

interact electrostatically with a hyper-polarized cytoplasmic layer of the plasma membrane.[35] KRAS4A contains two short palmitoylated polybasic regions,[36] which provide a dual-site sequence for membrane targeting. The membrane-targeting region of the C-terminal has Cys180, which goes through palmitoylation and independently enhances its association with the cell membrane.[37] PTM is crucial for the membrane association of KRAS4A and KRAS4B and helps predict different membrane attachment dynamics, which are essential for KRAS function.[38]

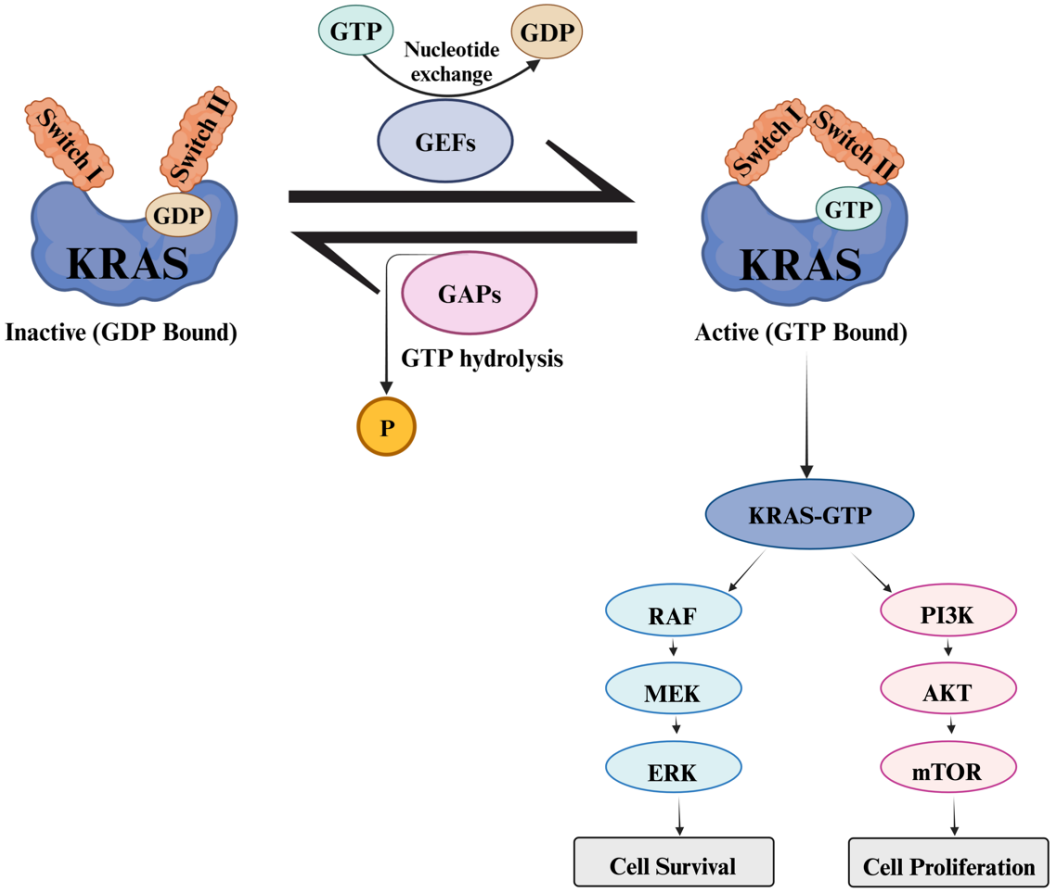

Figure 3: KRAS signaling pathway. The simplified diagram of KRAS signaling showed KRAS functioning as a molecular switch, cycling in an inactive state (GDP-bound) to an active state (GTP-bound) to control cell proliferation (PI3K) and survival (RAF).

2.2 KRAS switches between ON and OFF states

KRAS protein functions as a molecular switch regulating cell proliferation and progression by cycling between its inactive (GDP-bound) and active (GTP-bound) states. This dynamic cycling is fundamental to its role in transducing signals through key pathways such as PI3K/AKT, and MAPK/ERK pathways, which regulate cell proliferation survival (**Figure 3**).[39–41] KRAS activation

and inactivation are mediated through conformational changes mainly in the switch-I and II loops, which enable or inhibit interactions with downstream effector protein [42–44] s.

2.2.1 KRAS switch ON state

KRAS is activated upon GTP binding, which induces conformational changes that facilitate its interaction with downstream effector proteins (**Figure 3**). In response to the external signal, such as EGF binding to EGFR, the affinity of the KRAS-GDP complex decreases in the presence of GEFs, allowing GDP to be replaced by GTP, which has higher affinity and 10-fold higher cellular concentration than GDP.[45,46] GTP binding induces conformational changes in KRAS' switch I and II domains, enabling its interaction with downstream effector proteins like RAF kinases to initiate signaling cascades. The mechanism is mediated by conserved residues Thr35 and Gly60 in switches I and II, which form hydrogen bonds with the γ-phosphate of the GTP. These interactions stabilize GTP in position and maintain the two switch regions in the active conformation, facilitating effector protein binding.[47]

Guanine Nucleotide Exchange Factors (GEFs) trigger the KRAS shift from the OFF state to the ON state.[48] For instance, SOS1 (Son of Sevenless 1), a known GEF, facilitates the nucleotide exchange from GDP to GTP, and enables GTP to interact with the G-domain of the KRAS protein.[49,50] Once GTP binds, switches I and II undergo conformational changes to interact with effector proteins. Subsequently, transmission of the downstream signaling cascades promotes cell proliferation and survival.

Hydrolysis of GTP results conformational change in both switch domains rendering KRAS incapable of binding to effector proteins. This effectively shuts down the downstream signaling pathways, leaving KRAS in inactive state at the cell membrane.[51]

2.2.2 KRAS switch OFF state

KRAS inactivation is mediated through GTP hydrolysis. Intriguingly, KRAS hydrolyzes GTP slowly. GAPs (GTPase- Activating Proteins) like NF1 (Neurofibromin1) are crucial for strengthening the GTPase activity of KRAS. GAPs help stabilize GTP hydrolysis' transition state, thereby accelerating KRAS' inactivation.[45,49] The GDP OFF-rate is very slow ($t½$ = 6 min, K_{off} = 2 X 10^{-3} s^{-1} at 20^0C) due to the formation of stable hydrogen bonds between guanine of GDP and

residues Lys117, Asn116, Asp119, Ala146. This stability allows the RAS proteins to remain inactive until regulatory proteins produce the GTP/GDP exchange signal.[45]

2.2.3 Significance of KRAS Dynamics:

The conformational dynamics of KRAS are central to its function as a molecular switch, regulating intracellular signaling by alternating between GDP-bound (inactive) and GTP-bound (active) states. This switching mechanism is governed by three highly flexible regions within the G-domain: the P-loop (residues 10-14), Switch I (residues 30-40), and Switch II (residues 58-76). These regions undergo distinct conformational rearrangements in response to nucleotide binding and hydrolysis, which in turn dictate KRAS's ability to engage effectors such as RAF, PI3K, and RalGDS.

The conformational dynamics of wild-type and mutant KRAS proteins differ substantially, particularly in how mutations at codon 12 influence the stability of the active state. In wild-type KRAS, molecular dynamics simulations[42] reveal significant flexibility within the Switch I (residues 30–40) and Switch II (residues 58–76) regions, particularly in the absence of GTP hydrolysis. This flexibility underlies the protein's intrinsic ability to transition between GDP- and GTP-bound states. However, mutations such as G12C or G12D introduce side-chain steric interference within the nucleotide-binding site, which impairs GTP hydrolysis and biases KRAS toward a more persistent GTP-bound, active-like conformation. In the absence of inhibitors, these mutant forms exhibit greater fluctuations in inter-residue distances and increased mobility of the switch regions, suggesting a destabilization of the inactive state. Structural analyses further show that the G12 substitutions promote a partially open conformation of the nucleotide-binding pocket, facilitating effector engagement and downstream signaling. Thus, G12C and G12D mutations intrinsically stabilize the active state of KRAS by altering its conformational landscape.

2.3 Difference between KRAS, HRAS, and NRAS

RAS genes are evolutionarily conserved and exhibit high structural similarity. They share key functional properties, including the ability to bind and hydrolyze GTP, which is central to their role as molecular switches in cellular signaling. The KRAS, HRAS, and NRAS genes are widely expressed and conserved among species, though their expression levels vary by tissue and developmental stages.[52,53]KRAS, HRAS, and NRAS are located on chromosomes 12, 11, and 1, respectively.[7,54] These three genes code for four protein isomers, namely KRAS4A, KRAS4B,

HRAS, and NRAS which share a conserved G-domain but differ in the HVR region that dictates their distinct cellular localization and membrane association.[55,56]

The HVR of each RAS protein undergoes different modifications. For instance, KRAS4B has a lysine-rich region that interacts directly with anionic phospholipids to anchor it to the cell membrane, while HRAS and NRAS rely primarily on palmitoylation for membrane attachment, which affects their subcellular distribution and potentially influences signaling behavior.[57,58] KRAS is predominantly expressed in many tissues, whereas HRAS has more restricted expression, primarily in epithelial tissues.[59] NRAS is more broadly expressed, and plays an important role in the regulation of hematopoietic cells proliferation and survival.[60]

Mutations in RAS isoforms are implicated in a variety of cancers, with each isoform exhibiting a preference for specific cancer types. This distribution arises from their unique biological roles and tissue-specific expression patterns.[61,62] KRAS mutations are highly present in pancreatic, non-small cell lung, and colorectal cancer, making it a prevalent oncogenic driver.[7] HRAS mutations are less common and are typically found in head, neck, bladder, and thyroid cancers.[63–66] HRAS and KRAS mutations disrupt GTP hydrolysis, but HRAS has different mutation hotspots. NRAS mutations are frequently associated with melanoma, acute myeloid leukemia, and thyroid cancer. NRAS mutations result in continuous stimulation of MAPK/ERK and PI3K/AKT signaling pathways, driving the development of tumors.[53]

3. Development of Inhibitors Targeting KRAS G12 mutation

3.1 Inhibitors Targeting KRAS G12C Mutation

3.1.1 Challenges to develop G12C inhibitors

KRAS is the first and most frequently occurring oncogene discovered; however, the search for inhibitors that would bind directly to KRAS could not see any significant results due to their very high affinity for GTP. RAS proteins bind GTP with picomolar concentration. In comparison, kinases, which are an important class of drug targets in oncology,[67–70] bind ATP in micromolar concentrations. Thus, developing competitive inhibitors for RAS proteins was extremely hard. In addition, lack of prominent allosteric pockets, owing to the relatively smaller size of the protein, hindered drug discovery efforts.

The mutation in KRAS Glycine 12 (G12C) allows cells to escape the external growth control signaling. In combination with mutations in tumor suppressor genes such as p53, this

confers cells with uncontrolled replicative potential. Along with mutations in tumor suppressor genes like p53, this gives the cell uncontrolled replicative potential.[71] The G12C variant of KRAS is the most important oncogenic mutation found in human cancer.

3.1.2 Breakthrough discovery and development of ARS-853 and ARS-1620 as KRAS G12C inhibitors.

Although the G12D mutation occurs more frequently in all types of cancers, the Kevin Shokat lab strategically focused on G12C because the potential to covalently target the mutated cysteine with various electrophiles covalently. To identify initial hits, a 'tethering' library of about 500 compounds, developed by the Shokat lab for targeting cysteine, was screened against GDP-bound KRAS G12C (OFF-state) for cysteine modification.[72] Two hits identified were **6H05** and **2E07 (Figure 4)**. The X-ray crystal structure of **6H05** showed that the compound did not bind in the nucleotide-binding pocket. The authors named this pocket as S-IIP (Switch-II pocket). Since the GTP-bound 'ON' state is responsible for the oncogenic activity, the researchers screened the entire tethering library against GTP-bound KRAS G12C and identified no hits. Subsequent analysis revealed that the two hit compounds that bind to the 'OFF' state occupy a pocket which is occupied by Switch II residues in the 'on' state. Significantly, this work identified a new allosteric pocket in KRAS G12C, enabling mutant-specific targeting of GDP-bound KRAS G12C and preventing subsequent activation. Further optimization of **6H05** involved introducing stronger electrophiles, like acrylamide, which led to the identification of compound 1, as shown in **Figure 4**, which shows 100 % modification at 10μM after 24 hours.[72]

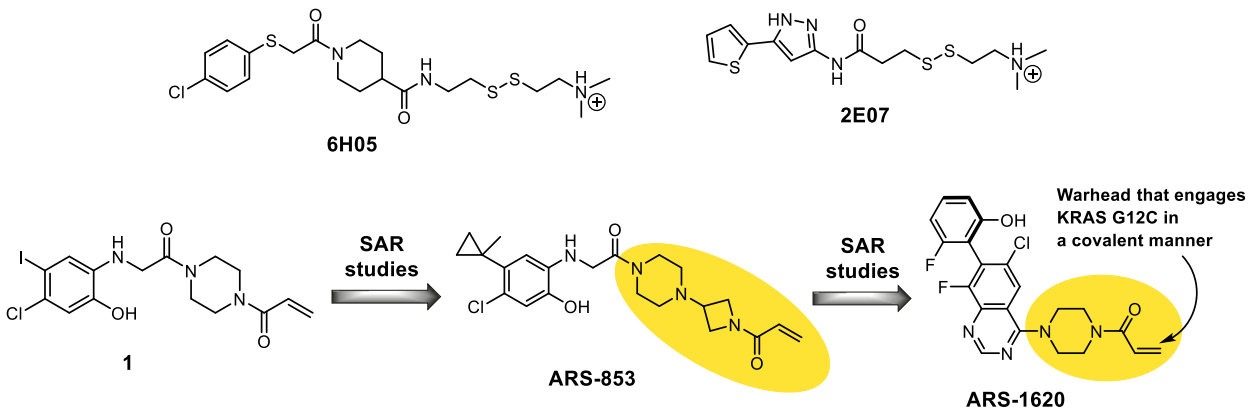

Figure 4: Optimization of **ARS-1620** through structure-based drug design. The acrylamide moeity forms covalent linkage with Cys12. ARS-853 was one of the early hits identified to directly bind to GDP-bound KRAS G12C. It shows no affinity for GTP-bound KRAS G12C.

California-based Wellspring Biosciences, founded by Dr. Kevan Shokat and colleagues, is based upon pioneering research into KRAS G12C inhibitors conducted by Dr. Shokat at the University of California, San Francisco. This research focused on KRAS G12C inhibitors that target the switch-II pocket. Patricelli *et al.* performed cellular studies with compound **1** in H358 cells and observed no protein modification, even at high concentrations of up to 100 μM.[73] Further SAR (structure activity relationship) studies were carried out to increase cellular modification. Although the SAR studies are not detailed, the authors identified and described a novel inhibitor **ARS-853**, which demonstrated 600-fold increased modification in biochemical study and a cellular IC_{50} of 1.6 μM. X-ray co-crystal structure of **ARS-853** in KRAS G12C confirmed the S-IIP (PDB ID 5F2E) binding of the inhibitor. However, like **1**, **ARS-853** exhibited no binding affinity to GTP-bound KRAS G12C.

Subsequently, Janes *et al.* from Well Spring Biosciences reported the further optimization of the scaffold to achieve in vivo efficacy.[74] **ARS-853** showed poor metabolic stability and oral bioavailability. Particularly, the *ortho*-phenol moiety and the glycine linker showed metabolic liabilities. In the SAR studies, the authors replaced the long flexible linker with a shorter and rigid bicyclic core, to occupy the region between Switch-II and α3 helix. A quinazoline moiety was identified as the best fit, and subsequently, a series of quinazoline-based KRAS G12C inhibitors with an acrylamide moiety to covalently engage the mutant cysteine was developed. Of this series of compounds, **ARS-1620** was identified as the best hit (**Figure 4**).

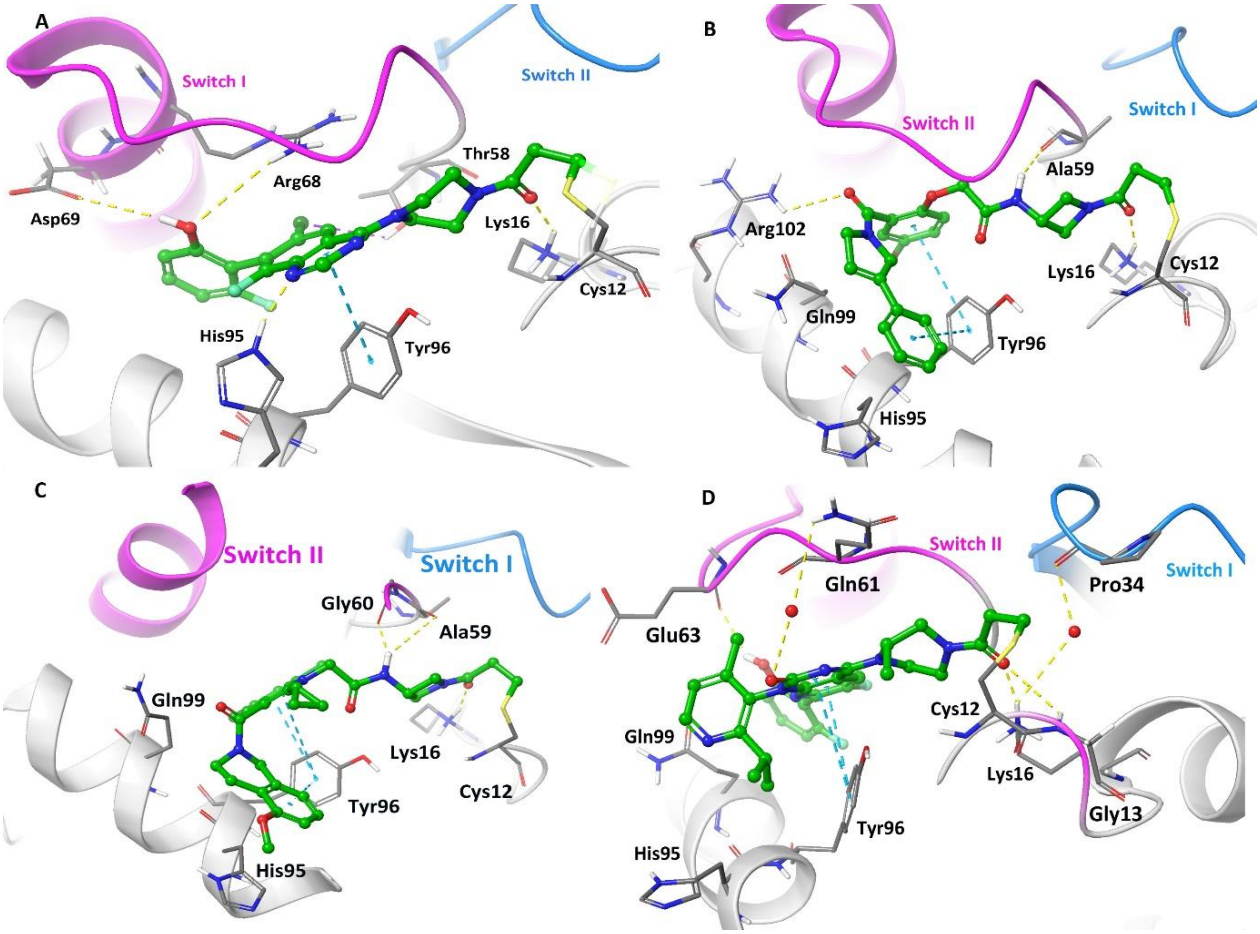

Figure 5: **A)** X-ray crystal structure of **ARS-1620** bound to KRAS G12C (PDB ID: 5V9U). **B)** X-ray crystal structure of compound **3** in KRAS G12C (PDB ID: 6P8X). **C)** X-ray crystal structure of compound **5** in KRAS G12C (PDB ID: 6P8Z). **D)** X-ray crystal structure of KRAS G12C bound to **AMG 510** (PDB ID: 6OIM). Hydrogen bonds are illustrated in yellow, and π-π stacking interactions in blue.

As expected, the X-ray crystal structure of **ARS-1620** showed the compound occupying the switch-II pocket and engaging Cys12 in covalent linkage (PDB ID:5V9U) (**Figure 5A**). A key interaction with His95 was also identified, which was missing in the **ARS-853** series of compounds. The biaryl moiety was stabilized by the presence of the two fluorines, a hydroxyl and a chlorine, resulting in atropisomers, of which the *S*-atropisomer showed 1000-fold greater potency than the *R*-atropisomer. The quinazoline moiety forms a π-π bond with Tyr96 and also a water-mediated hydrogen bond with its hydroxyl group. The carbonyl of acrylamide forms a hydrogen bond with Lys16. The OH group on the terminal fluorophenol engages in water-mediated hydrogen bonding with multiple residues.

Cellular studies of **ARS-1620** identified that covalent modification of KRAS G12C was most predominant in a proteomic screen spanning about 3000 proteins with cysteines. The compound showed enhanced oral bioavailability (F > 0.6), significantly improving compared to **ARS-853**. Further, it showed significant target occupancy and dose-dependent tumor growth inhibition in mouse xenograft models. Overall, while the discovery of **ARS-853** demonstrated the cellular potency of KRAS G12C inhibitors, the discovery of **ARS-1620** represented a major advancement in the development of direct KRAS inhibitors by demonstrating in-vivo efficacy.

3.1.3 Amgen's work in collaboration with Carmot therapeutics

Amgen reported a novel KRAS inhibitor developed using Carmot Therapeutics' Chemotype Evolution Technology, which facilitates rapid access to novel chemical diversity.[75] This technology involves a reactive functional group-containing 'bait' molecule systematically linked to compounds within Carmot's proprietary fragment library. This process facilitates rapid generation of a compound library, synthesized at the nanogram scale and evaluated for biological activity without purification. Subsequently, active compounds (hits) identified through screening are resynthesized at a milligram scale, purified, and subjected to for further studies. Following this strategy, a library of 3300 compounds was synthesized using *N*-(1-acryloylazetidin-3-yl)-2-bromoacetate as the initial '**bait**' molecule and screened against KRAS G12C (**Figure 6**). Compound **2** was identified as a promising hit, with its covalent binding to Cys12 confirmed via mass spectrometry. The binding pose of compound **2** in KRASG12C was determined using X-ray crystal studies.

To enhance potency, second-generation baits were designed leading to the identification of two key structures: 1) a phenol bait and 2) an indole bait. Subsequent screening of 2,600 compounds synthesized with the phenol bait yielded compound **3**, which demonstrated 10-fold enhanced potency compared to compound **2**. Parallelly, 2900 compounds with the indole bait were synthesized and screened, of which, compound **4** was identified as the most active with 100-fold greater potency compared to **2**. Structure optimization of compound **4** proceeded via two distinct phases. Initial exploration of indole position 3 substitutions, involving a small library of approximately 10 compounds, yielded no significant improvements. Subsequently, exploration of indole positions 2 and 5, led to the identification of compound **5** (**Figure 6**). X-ray crystallographic analysis of both **3** and **5** revealed that their increased potency is due to optimal occupancy of the binding pocket formed by His95, Tyr96, and Gln99 (**Figure 5B** and **5C**).

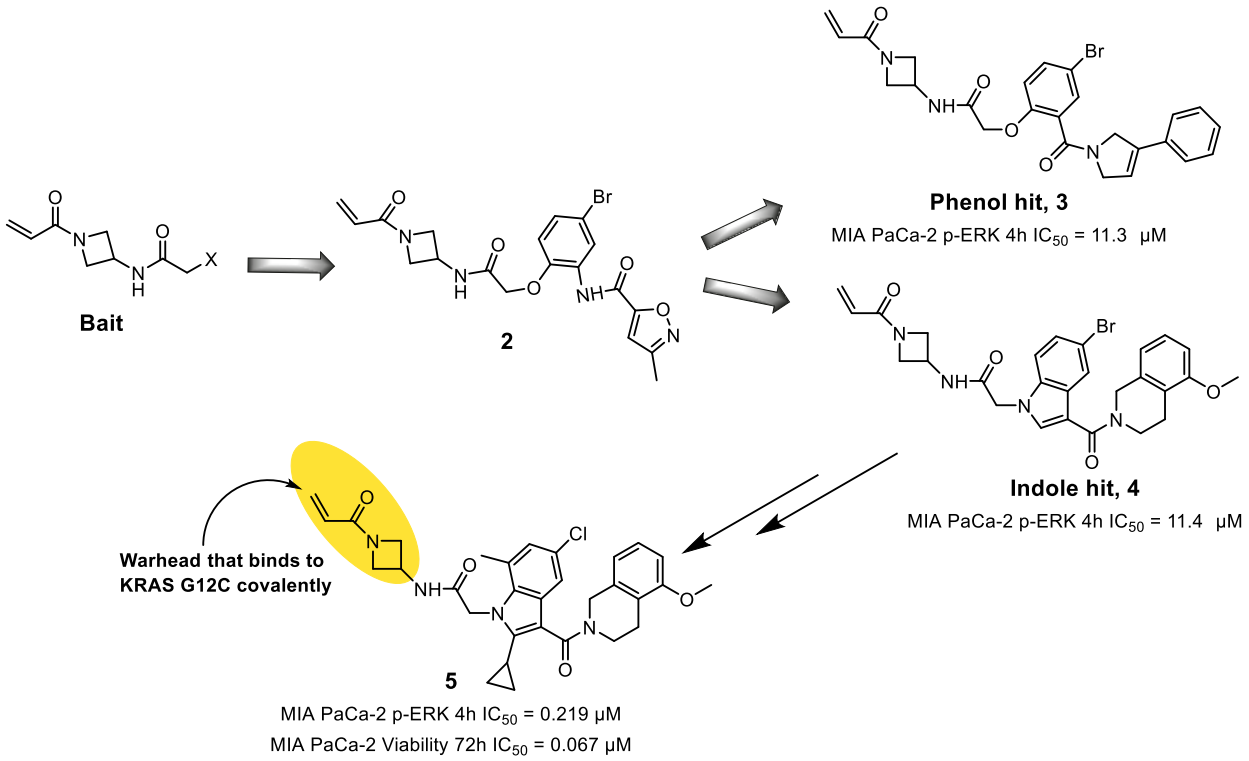

Figure 6: Optimization of compound **5** through structure-based drug design. Phenol and indole baits were designed with an acrylamide moeity to engage Cys12. Compound libraries based on these baits were synthesized and screened to identify hit compounds. X-ray crystal structure of the hit compounds identified a crytpic binding pocket formed by His95, Tyr96, and Gln99.

The structural findings from this work provided critical insights that guided the design of subsequent compound series, ultimately leading to the development of **Sotorasib** (**AMG 510**). The key structural elements identified in these studies, particularly the critical interactions within the His95-Tyr96-Gln99 pocket interactions, proved instrumental in optimizing both the potency and pharmacological properties of later generations of KRAS G12C inhibitors.

3.1.4 Discovery and Development of Sotorasib (AMG 510)

Amgen discontinued the indole-based lead compound **5** due to its poor oral bioavailability. The findings of this work lead to the identification of sotorasib which was described in a 2020 publication from Amgen.[76] The researchers aimed to modify the structure of **ARS-1620** to occupy the His95 cryptic binding pocket. Analysis of the X-ray crystal structure of **ARS-1620** indicated that N1 position substitutions could occupy the target pocket. A key challenge was compensating

for the loss of hydrogen bonding at the *N*1 position with additional interactions. The researchers first replaced the quinazoline group of **ARS-1620** with a phthalazine group while maintaining crucial hydrogen bonding. A phenyl group was introduced at the C-4 position to occupy the target pocket. Although there was a significant loss of potency, the X-ray crystal structure confirmed that the phenyl group was oriented toward the His95 pocket. Aliphatic substitutions at the ortho-position of the C4-phenolic group improved biochemical and cellular potency. An isopropyl substitution at the ortho position in compound **6** was optimal, yielding comparable potency to **ARS-1620 (Figure 7)**. Next, the *N*3 of phthalazine was replaced with a carbonyl (-C=O) to afford quinazolinone moiety, which showed several-fold increased potency compared to **ARS-1620**. This series of compounds exist as atropisomers, and the authors identified through X-ray crystal that only the *R*-atropisomer (compound **7**) was active. Thus, the further SAR focused exclusively on this isomer. The authors hypothesized that the reduced permeability could be due to an increased desolvation penalty, and to compensate, nitrogen was introduced in the biaryl ring at position 8 (compound **8**) to facilitate intramolecular hydrogen bonding. Further studies included exploring substitutions on the piperazine group and the fluorophenolic moiety. Notable results from the substitutions on the piperazine group included the addition of a methyl group, which not only improved the cellular potency but also bioavailability. Interestingly, removing the phenylic OH did not affect the potency but improved MDCK permeability. Overall, the resulting compound **9** showed improved MDCK permeability, and enhanced potency, and superior oral bioavailability.

A final challenge encountered in this study was the slow interconversion of atropisomers. For compound **9**, a slow interconversion from *R* to *S* isomer was observed with a half-life of about 8 days. The further optimization focused on restricting biaryl bond rotation to slow this interconversion. This led to the discovery of compound **11** (**Sotorasib**/**AMG 510**), which showed a racemization half-life exceeding 180 years.[76] It is the first-in-class G12C-targeted KRAS inhibitor shown to be effective for tumor regression in in vitro and in vivo studies. Studies expanded to include other types of standard chemotherapy and immune-checkpoint inhibitors, demonstrating strong immunological responses and extended therapeutic effects in syngeneic models.[77,78]

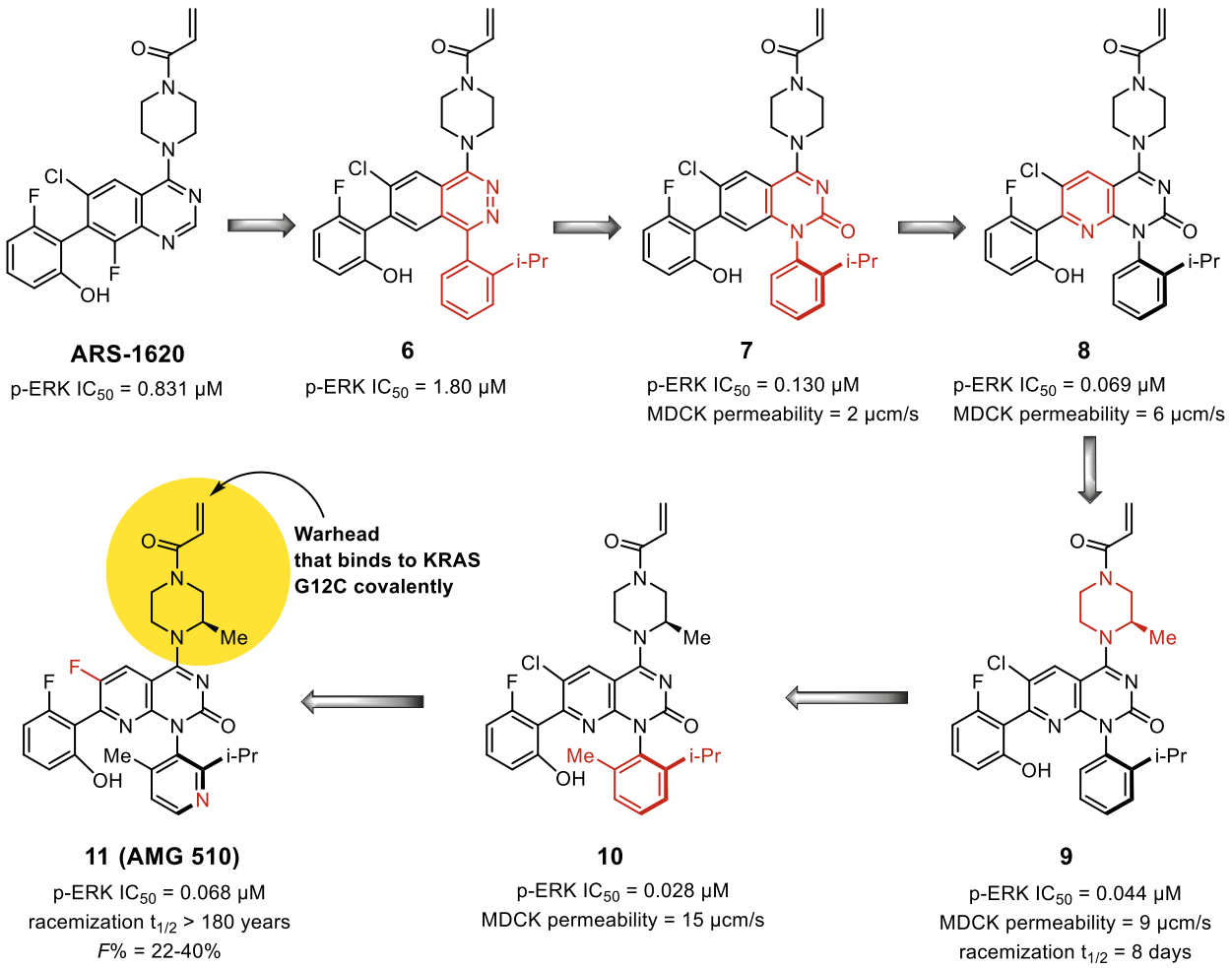

Figure 7: Further optimization of **ARS-1620** resulting in discovery of **AMG510** (compound **11**) through structure-based drug design. Substitutions on biaryl moeity lock the rotation of C-N bond resulting in atropisomers. **AMG510** is the first FDA approved direct KRAS inhibitor.

The co-crystal structure of **Sotorasib** (**AMG 510**) in KRAS G12C, reported by Canon et al. (**Figure 5D**)[79] revealed that the acrylamide moiety covalently interacts with Cys12. The carbonyl group of acrylamide forms hydrogen bonds with Lys16 and Gly13, while the isopropyl moiety on the pyridine ring occupies the H95 cryptic pocket and forms several strong hydrophobic interactions with Tyr96. The azaquinazoline ring forms two π-π interactions with Tyr96, and the hydroxyl group of fluorophenolic moiety engages in a hydrogen bond with the backbone of Glu63. Together, these interactions contribute to the strong binding and inhibition of KRAS G12C.

AMG-510 binding to KRAS G12C significantly reduces conformational flexibility and stabilizes key structural elements of the protein. Molecular dynamics simulations[42] revealed that in the absence of AMG-510, Switch II residues such as Thr58, Gln61, Glu63, and Arg68 exhibit substantial fluctuations, with RMSF values exceeding 1.0 Å. Upon covalent attachment of AMG-

510, these fluctuations markedly decrease; Thr58, Glu63, and Arg68 display enhanced stability in both spatial positioning and torsional profiles. Inter-residue Cα distances, including Val14-Tyr64 and Asp30-Glu62, also remain stable throughout the 1 μs simulation, highlighting the inhibitor's ability to constrain the Switch II loop and adjacent regions, thereby reinforcing the GDP-bound inactive conformation of KRAS G12C.

Following successful clinical trials, **Sotorasib** (**AMG 510, Lumakras®)** received accelerated approval from the FDA in 2021 and full approval on December 26, 2023, for adult patients with KRAS G12 -mutated locally advanced or metastatic non-small cell lung cancer. The approval was based on the multi-center phase III trial NCT03600883, which reported the median progression-free survival of 7 months, and the median overall survival of 13 months.[80] While these results may be considered modest, and there is still room for therapeutic improvement, the approval of **Sotorasib** represents a landmark achievement, as it is the first KRAS inhibitor to received FDA approval after decades of drug discovery and development targeting KRAS.

3.1.5 Discovery and Development of Adagrasib (MRTX849)

Following the discovery of the Switch-II pocket by the Shokat lab, Mirati Therapeutics conducted a library screening of covalent fragments to identify a hit compound capable of covalent modification of Cys12, which resulted in the discovery of compound 12.[81] X-ray crystal structure of compound **12** in complex with KRAS G12C (PDB ID: 6N2J) revealed several key interactions (**Figure 9A)**: 1) a covalent bond between the acrylamide moiety and Cys12, 2) hydrogen-bonding networks between the carbonyl of acrylamide and Lys12, and 3) between N1 of the pyrimidine and His95, 4) naphthyl ring is buried in a relatively hydrophobic pocket surrounded by Val9, Ile100, Phe78, Tyr64, and Met72. In the first cycle of SAR studies (**Figure 8**), the authors synthesized 5 compounds designed to form a hydrogen bond with proximal Asp69. Of these, only the naphthalene derivative (compound **13**) with 3-hydroxy substitution demonstrated significant protein modification and H358 cell growth inhibition. Subsequent SAR studies focused on the C-2 position of pyrimidine to establish interactions with Glu62 and to reduce activity against EGFR, resulting in compound **14.** X-ray crystal structure indicated that compound **14** retained the interactions of compound **13** while establishing additional contacts, such as the naphthol hydroxyl forming a hydrogen bond with Asp69, and the C-2 basic amine substituent interacting with Glu62

(Figure 9B and **9C)**. Compound **14** shows robust protein modification around 84% at 3 µM and potent antiproliferative activity against H358 cells (IC_{50}/GI_{50} = 70 nM).

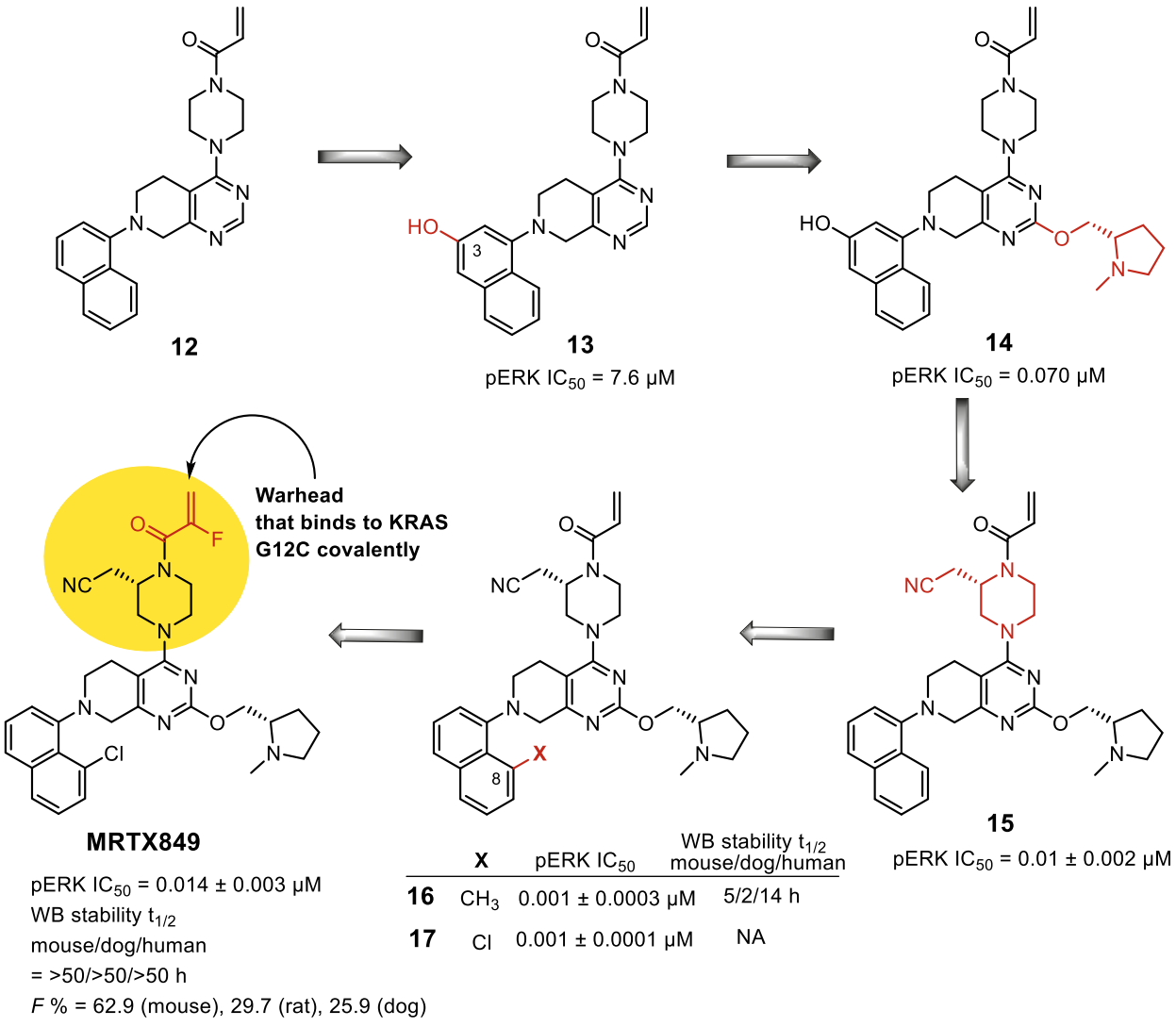

Figure 8: Optimization of **MRTX849** through structure-based drug design. Adagrasib (MRTX849 is an oral, selective KRAS G12C inhibitor approved for treating KRAS G12C-mutated non-small cell lung cancer (NSCLC) and, in combination with cetuximab, for colorectal cancer. It is the second direct KRAS inhibitor approved by FDA

Although compound **14** showed potent inhibition, it suffered from poor pharmacokinetic properties. Specifically, the phenolic OH of naphthol resulted in extensive Phase II metabolism. Removing the phenolic OH in compound **14** improved the clearance and oral bioavailability but significantly decreased the cellular pERK inhibitory potency. X-ray crystal structure (PDB ID 6USX) revealed crystal water in the vicinity of the piperazine moiety, forming a hydrogen bond network with Gly10 and Thr58. The authors hypothesized that displacing this water could result

in a significant gain in potency. A few analogs were synthesized with substitutions on the piperazine carbons, of which the racemic mixture of compound **15** showed about 10-fold improved activity compared to compound **14**. Further analysis revealed that only the S-enantiomer (compound **15**) showed activity with cellular pERK IC_{50} of 10 ± 2 nM. Compound **15** also showed favorable ADME properties. X-ray crystal structure of compound **15** (PDB ID 6USZ) showed a small pocket that appropriate substitutions on C8 of naphthalene ring could occupy. Six analogs were synthesized with various substitutions on C8 of the naphthyl group, of which chloro and methyl groups showed low nanomolar potencies. In-vivo studies of these two compounds indicated lower bioavailability that could be arising from conjugation with GSH. To decrease this, substitutions were introduced in the acrylamide group, which resulted in the identification of **MRTX849** (**Figure 8**). The X-ray crystal structure of **MRTX849** in KRAS G12C (**Figure 9D**) showed all the interactions established during the lead optimization process.[82] The K_{inact} and K_i values for MRTX849 determined from three separate experiments were 0.13 ± 0.01 s^{-1} and 3.7 ± 0.5 μM, respectively. The K_{inact}/K_i value for MRTX849 was calculated to be 35 ± 0.3 mM^{-1} s^{-1} compared to other KRAS G12C inhibitors, **ARS-1620** (1.1 mM^{-1} s^{-1})[83] and **AMG 510** (9.9 mM^{-1} s^{-1})[84] Although MRTX849 shows lower potency (pERK IC_{50} of 14 nM) compared to compound **16** and **17**, it demonstrated excellent $t_{1/2}$ in whole blood (WB) stability assay in mice, dogs, and humans. Eventually, **MRTX849** was identified as a specific KRAS G12C inhibitor possessing enhanced drug-like properties.[85] This study elucidated the various mechanisms that attenuate antitumor activity, such as KRAS nucleotide cycling and feedback pathways. The study elucidated resistance mechanisms, including RTK activation, KRAS dependence bypass, and disruption of cell cycle homeostasis. In the most resistant models, **MRTX849** demonstrated enhanced responses and tumor regression when combined with other agents targeting RTK, mTOR, or the cell cycle.[85–87]

Following successful in vivo studies, **MTRX849** (**Adagrasib,** marketed as **Krazati®**) proceeded to clinical trials. The compound showed efficacy in clinical trials and received accelerated approval by the FDA in December 2022 for treatment of KRAS G12C-mutated metastatic or locally advanced NSCLC. A second accelerated approval was awarded in June 2024 for combination therapy with cetuximab for KRAS G12C mutated colorectal cancer.[88]

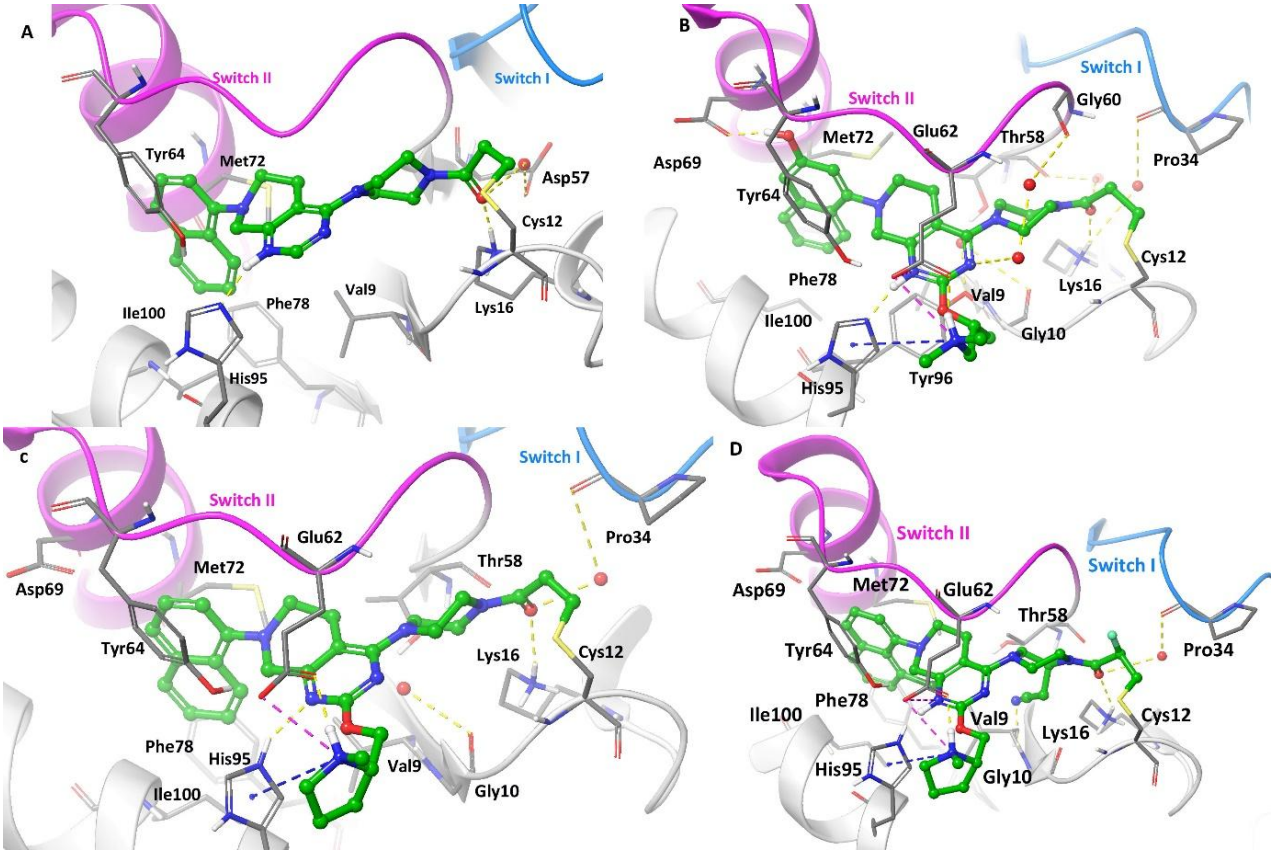

Figure 9: **A)** X-ray crystal structure of Compound **12** bound to KRAS G12C (PDB ID: 6N2J). **B)** X-ray crystal structure of compound **13** in KRAS G12C (PDB ID: 6N2K). **C)** X-ray crystal structure of compound **14** in KRAS G12C (PDB ID: 6USX). **D)** X-ray crystal structure of KRAS G12C bound to **MRTX849** (PDB ID: 6UT0). Hydrogen bonds are illustrated in yellow and π-π stacking interaction in blue.

It is significant to note that His95 in KRAS is a key determinant of isoform selectivity in covalent KRAS(G12C) inhibitors. A study reported by Mahran et al[89] demonstrated that adagrasib forms strong and specific interactions with H95, through hydrogen bonding and cation–π interactions, resulting in high affinity and specificity for KRAS. These interactions are absent when His95 is substituted with leucine, as seen in NRAS, or glutamine, as in HRAS, leading to markedly reduced binding of adagrasib to non-KRAS isoforms. Conversely, sotorasib showed minimal dependence on H95 for its binding; instead, it maintains a relatively consistent interaction profile across KRAS, NRAS, and HRAS. This renders sotorasib an isoform-agnostic inhibitor capable of targeting G12C mutations in all RAS isoforms. Functional assays confirmed that mutations at His95 significantly impair adagrasib's activity but have only marginal effects on sotorasib. This distinction is clinically relevant, as sotorasib is therapeutically beneficial in rarer NRAS(G12C) cancers[90] and possibly in HRAS(G12C) cancers, while adagrasib is limited to KRAS-specific targeting.

3.1.6 Discovery and Development of Opnurasib (JDQ443)

A 2022 study from Novartis reported the discovery of **Opnurasib** (**JDQ443**), a novel covalent KRAS G12C inhibitor that binds in the switch-II pocket.[91] The initial hit, compound **18**, was obtained from screening an in-house library of covalent compounds. The dimethyl substitution on the central pyrazole ring and the 5-methyl substitution on indazole hinder the axial rotation, resulting in atropisomerism. Structure-activity relationship studies identified that only the eutomer shows KRAS G12C protein modification, whereas the distomer shows no potency. Thus, further research was focused only on the potent isomer. The co-crystal structure of compound **18** (**Figure 14A**) in KRAS G12C was solved (PDB ID: 7R0Q), which revealed that the acrylamide moiety was positioned towards Cys12, and the carbonyl amide formed hydrogen bonds with Lys16 and Gly60, as expected. The N1 of indazole forms a hydrogen bond with Asp69, and the bicycle system occupies the adjacent hydrophobic pocket. The methyl group on pyrazole occupies a small hydrophobic pocket surrounded by Val9, Thr68, and Met72, as shown in **Figure 14A**.

Since an overly reactive acrylamide moiety tends to form non-specific covalent adducts, in the initial SAR studies, they aimed to balance specific KRAS G12C reactivity and intrinsic reactivity, measured by $t_{1/2}$ in glutathione assay. Several substitutions were introduced on the acrylamide containing phenyl ring. However, the best results were observed when the phenyl ring was replaced by spiroazetidine (compound **19**). Exploration of the 3-position of pyrazole revealed that introducing cyclohexyl at this position (compound **20**) maintained specific reactivity, indicating tolerance of bulkier groups at this position. Replacing the C-5 methyl group on indazole with chlorine showed a 3-fold increased reactivity. Introduction of a methyl group at the 6-position of indazole resulted in further potency enhancement in both enzymatic and cellular studies. The proximity of the cyclohexyl group to His95 revealed an opportunity for potential interactions. Subsequently, the cyclohexyl group was replaced with a phenyl moiety, and co-crystallography of compound **21** revealed a π-π interaction with His95, a novel finding, as previous efforts established directional hydrogen bonds with His95, rather than π-π interaction. Compound **21** showed high potency (pERK IC_{50} of 40 nM). In vivo models of **21** showed a relatively short half-life of (2.5 hours) and moderate tumor size reduction, indicating the moderate therapeutic potential of the scaffold.

To enhance in vitro and in vivo activity, further SAR studies explored the C-3 position by replacing the phenyl group with various bicyclic moieties. Incorporation of indazole significantly

improved potency, which was further enhanced by N1-methyl substitution, leading to **JDQ443** (**Figure 10**). Crystal structure of **JDQ443** in KRAS G12C (**Figure 14B**) indicated that substitutions at N1 and N2 of indazole are well occupied in the binding pockets. Subsequent aliphatic substitutions were introduced to improve the pharmacokinetic properties.[91] However, modifications that increased aqueous solubility compromised membrane permeability, while those enhancing membrane permeability reduced aqueous solubility.

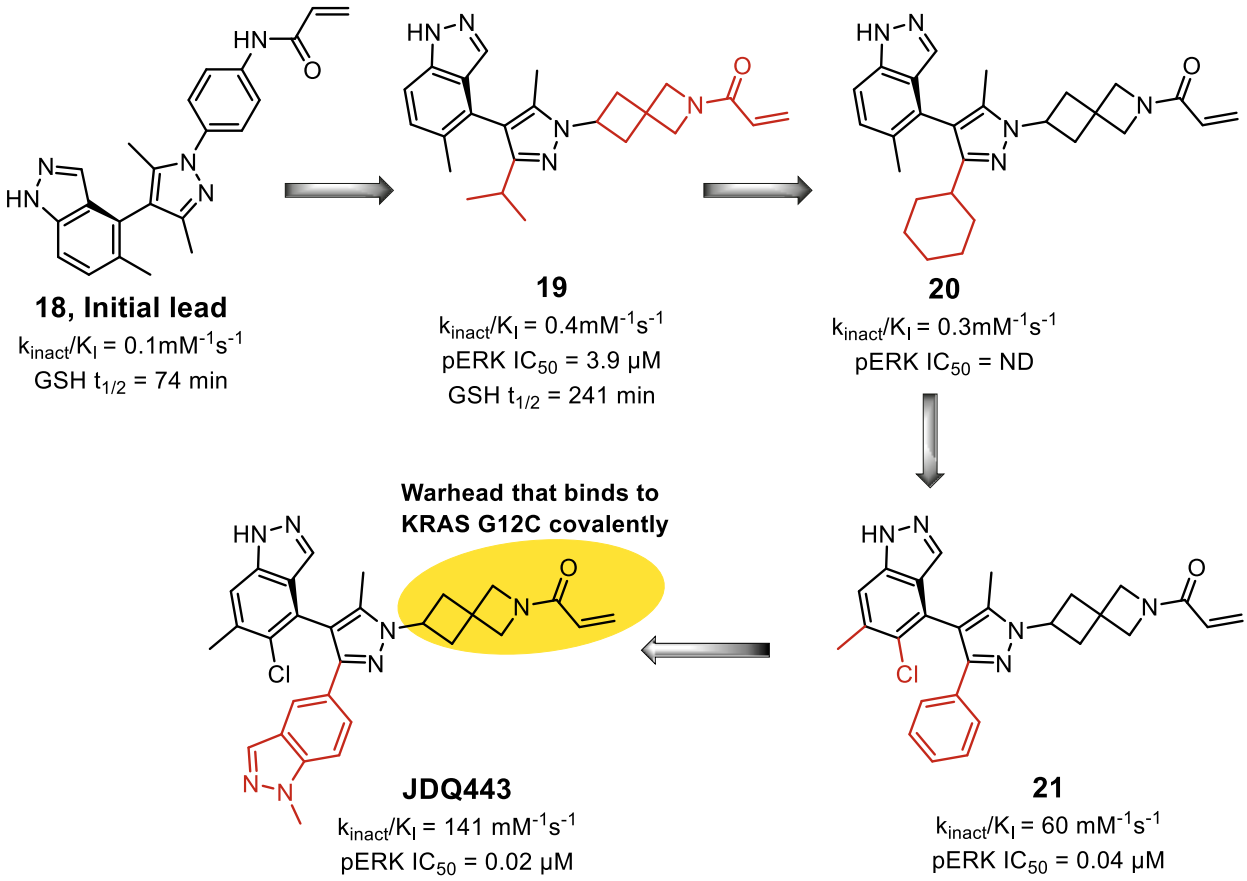

Figure 10: Optimization of **JDQ443** from an indazole-based. X-ray crystal studies identified tolerance to bulkier substitions on pyrazole ring. Together with optimization of the acrylamide, JDQ443 (opnurasib) was identified and is currently in Phase I and II clinical trials.

JDQ443 demonstrated good in vivo efficacy and pharmacokinetic properties in mouse and dog models. **JDQ443** (**Opnurasib**) is currently being evaluated in Phase I and II clinical trials in patients with advanced solid tumors harboring KRAS G12C mutation (NCT04699188, NCT05445843, NCT05132075).

3.1.7 Discovery and development of GDP mimetic inhibitors targeting *KRAS G12C*

Dr. Nathanael Gray's lab reported compound **22**, a GDP mimetic inhibitor with a chloroacetamide moiety that forms a covalent linkage with Cys12 of KRAS G12C (**Figure 11**).[92] However, **22** contains multiple charged phosphate groups that hamper its membrane permeability. The Gray group attempted caging strategies to mask the charged phosphates group but were unsuccessful due to compound instability.[93] As part of SAR studies to identify better compounds, various bisphosphonate isosteres were synthesized. In the ActivAlpha assay, compound **22** showed K_I = 9 nM. Replacing the central oxygen of the bisphosphonate linker with methylene resulted in compound **23**, which showed a 300-fold reduction in K_I activity. This decrease in activity indicates the importance of the central oxygen atom and its interactions with P-loop residues of KRAS. Next, the Gray group fluorinated the methylene group in compound **24** (K_I = 0.38 μM, which showed a 7-fold enhanced affinity for KRAS compared to **23** (K_I = 2.7 μM). More importantly, compounds **23** and **24** demonstrated improved chemical stability, with K_{inact}/K_I values of 0.02 and 0.9 $min^{-1}.\mu M^{-1}$ respectively, compared to **22**, which had K_{inact}/K_I value of 95 $min^{-1}.\mu M^{-1}$. Subsequent attempts to replace one of the bisphosphonates with a sulfonamide moiety (compound **25**) did not improve the results compared to the lead compound. The X-ray crystal structure of **22** reveals a hydrogen bond between the linker amide group and Lys16. However, the β-phosphate of **22** engages with magnesium ion and its coordinated water network. The magnesium-mediated interaction between the β-phosphate and Tyr32 is evident in compound **22**. Also, hydrogen bonding is observed with P-loop residues Gly15 and Lys16.

This work concluded with a promising lead, compound **24** (**Figure 11**), featuring a difluoro methylene bisphosphonate moiety, which can facilitate easier prodrug development. Although showing a 40-fold reduction in affinity compared to **22**, it demonstrates superior chemical stability by avoiding the instability issues associated with the phosphate anhydride bond.[92]

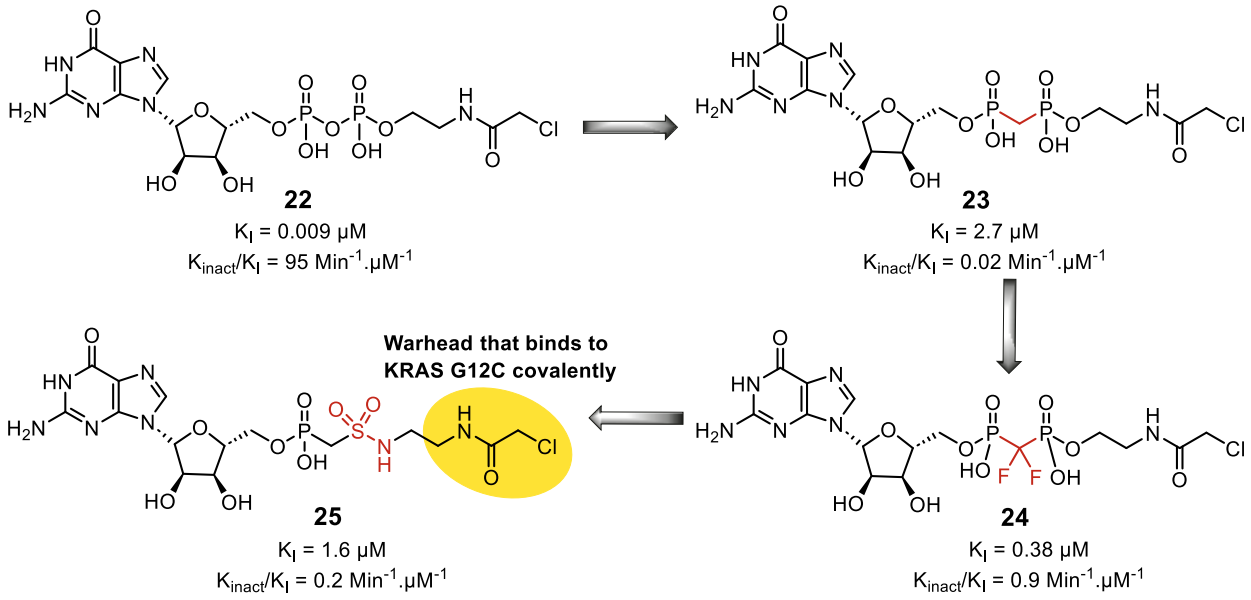

Figure 11: Optimization of **GDP mimetic inhibitors** through structure-based drug design.

3.1.8 Discovery and development of ASP6918

A 2022 report from Tsukuba Research Center, Japan disclosed a series of quinazoline based KRAS G12C covalent inhibitors.[94] Compound **26** was identified as the initial hit with IC_{50} of 0.47 µM in a cell-free KRAS G12C inhibition assay. During SAR studies, the piperazine linker was replaced with various spiro moieties (**Figure 12**). While compound **28** showed a 3-fold improvement in potency, it suffered from decreased $t_{1/2}$ in the GSH trapping test. However, compound **27** showed similar $t_{1/2}$ like compound **26** and a slight improvement in potency (IC_{50} = 0.35 µM). The pERK inhibition in the H1373 cell line of the modified compounds remained comparable to the lead, with **27** showing slight improvement. Compound **27** also showed improved cell growth inhibition (GI_{50} = 0.39 µM) of H1373 compared to compound **26** (GI_{50} = 0.65 µM). Replacing the NH linker with oxygen at the C-2 position of the quinazoline ring resulted in a 5-fold enhancement in potency, while replacing it with sulfur attenuated the activity. Modification of the spiro-piperidine ring with other alkoxy derivatives showed no potency. Compounds **29** and **30** showed enhanced KRAS G12C inhibition, pERK inhibition in H1373 cells, and cell growth inhibition in H1373 cells (**Figure 12**). Notably, the compounds' lack of potency in A375 cells suggests their H1373 activity is arising from interfering in KRAS G12C signaling interference.

X-ray crystallographic analysis of compound **30** in complex with KRAS G12C was also solved by the authors (PDB ID: 7YCE) (**Figure 14C**). As expected, the acrylamide moiety forms

a covalent linkage with Cys12 residue. The binding is stabilized by three hydrogen bonds and a salt bridge: specifically, the carbonyl oxygen of acrylamide and Lys16, N1 of quinazoline and His95, and N1 of indazole with the sidechain carboxylate of Asp69. Additionally, a salt bridge formed between the piperidine nitrogen and the sidechain of Asp92. As illustrated in **Figure 14C**, the binding mode is further stabilized by aromatic H-bonds and CH-π interactions.

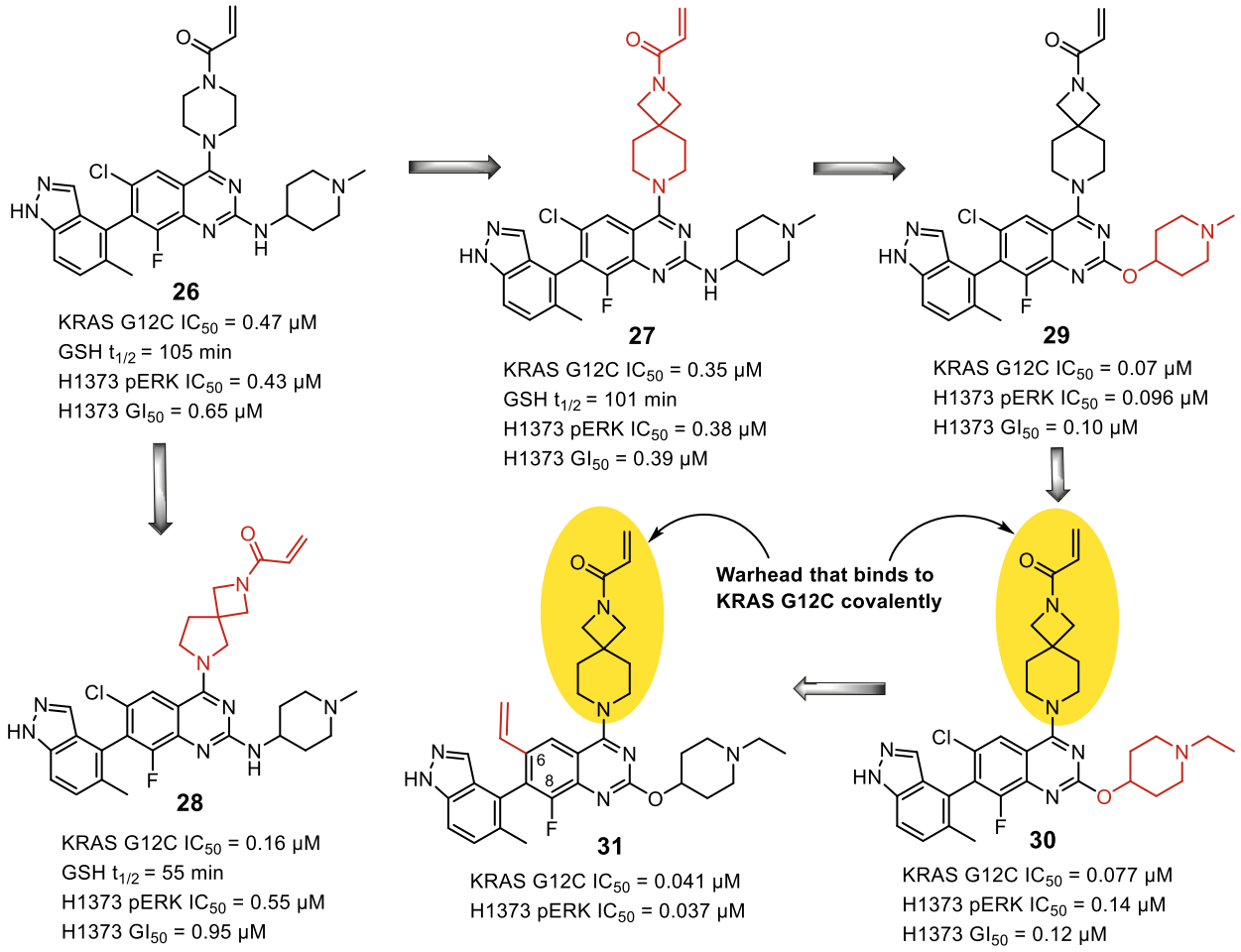

Figure 12: Optimization of compound **30** and **31** from quinazoline based hit compound. This work laid the foundation for identification of ASP6918.

In the 2024 follow-up report, they explored further SAR by modifying the substitutions at positions 6 and 8 on the quinazoline of compound **30**.[95] Replacing chlorine at C6 position with small alkyl groups of which allyl substitution showed the best KRAS G12C inhibition (compound **31**, KRAS G12C IC_{50} = 0.041 μM). Introducing a phenyl group at this position completely abolished activity, indicating the intolerance for bulkier substitutions. Next, the substitutions at the C-8 position were explored. Replacement of fluorine with hydrogen and cyano group resulted in a

significant loss of KRAS G12C inhibition while introducing an ethoxy group (compound **32**) at this position showed a 2-fold increase in potency for both KRAS G12C inhibition and pERK inhibition in the H1373 cell line (**Figure 13**). The combining substitutions of the C6 position (compound **31**) and C8 position (compound **32**) of quinazoline, along with replacing 1-ethyl piperidine with 1-methyl piperidine at the C2 position resulted in highly potent compounds (**33-35**). Increasing the bulk of the alkoxy group to ethoxy, cyclopropyl, or cyclobutyl groups maintained comparable potency. The most potent compound, **34**, exists in atropisomers like other KRAS G12C inhibitors. Atropisomers usually have different pharmacological activities due to the difference in interaction with Asp69. Therefore, they performed optical resolution on the promising compound **34** to separate the two atropisomers and evaluated their respective inhibitory activities. One of the atropisomers was identified as **ASP6918** (**Figure 13**), showed superior in vitro activity compared to the other atropisomer.

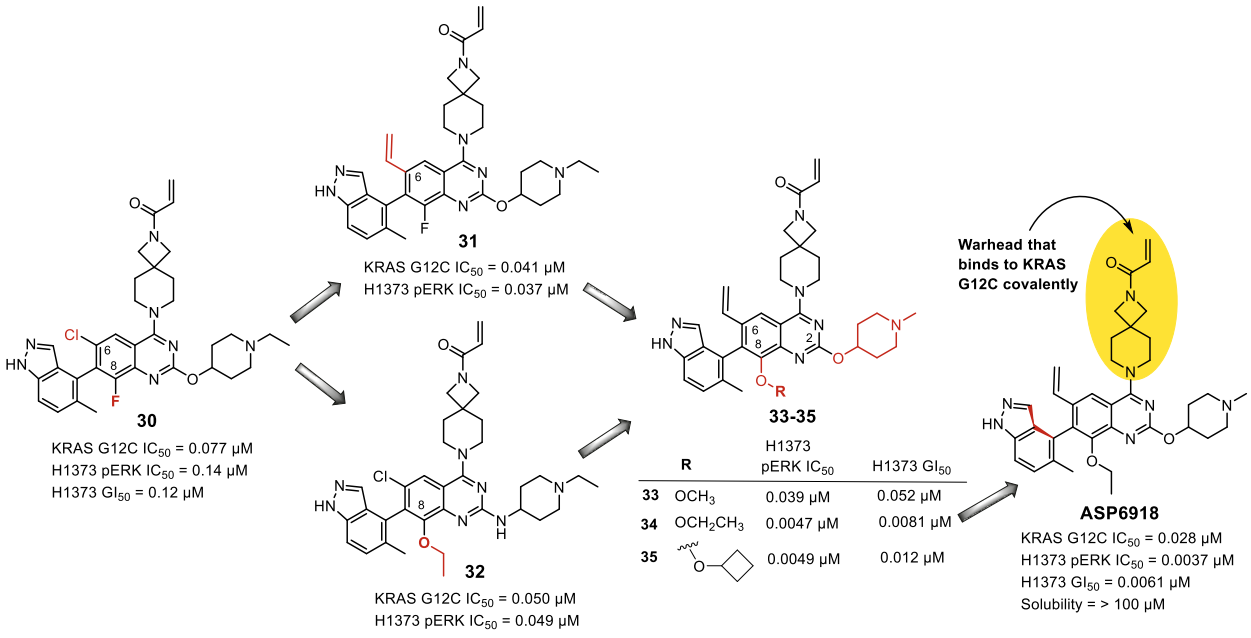

Figure 13: Optimization of **ASP6918** from compound **30**. Several substitutions on the quinazoline core were optimized to improve not only potency and in-vivo effcicacy but also pharmacokinetic properties.

The authors solved the crystal structure of the atropoisomer **ASP6918** in complex with KRAS G12C (**Figure 14D**) (PDB ID: 8X6R). The protein-ligand interactions observed were similar to those of compound **30**. The acrylamide forms a covalent linkage with Cys12. The salt

bridge with Asp92 and the three hydrogen bonds with Lys16, Asp69, and His95 were also retained as shown for compound **30**.

In-vivo studies on the lead compound were performed. At 3mg/kg dose, about 82% of tumor growth inhibition was reported, while treatment with 10 mg/kg resulted in significant tumor regression. The authors reported that further work on this scaffold would be to improve the pharmacokinetic properties of the lead compound.

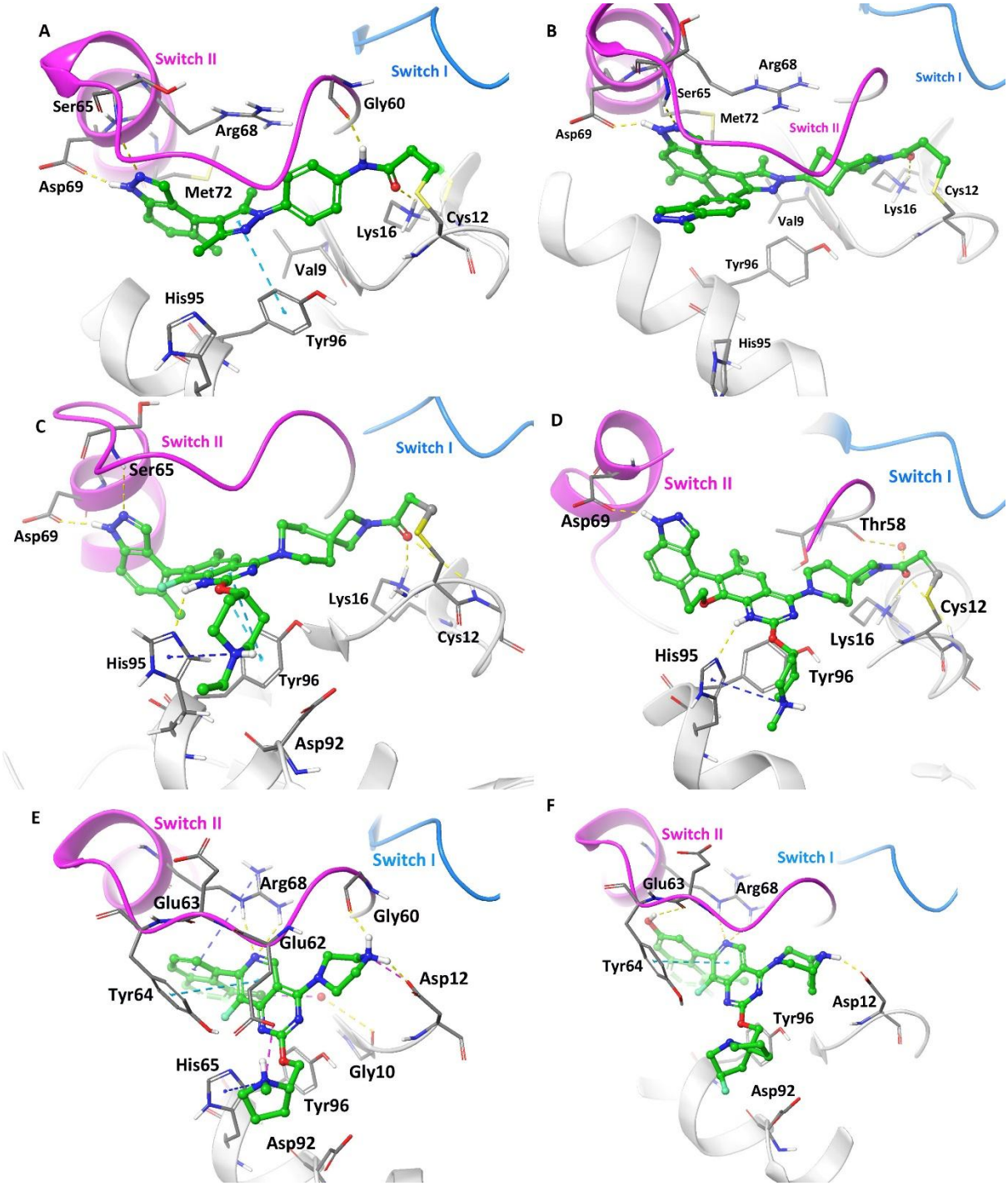

Figure 14: **A)** X-ray crystal structure of compound **18** bound to KRAS G12C (PDB ID: 7R0Q). **B)** X-ray crystal structure of **JDQ443** in KRAS G12C (PDB ID: 7R0M). **C)** X-ray crystal structure of compound **30** bound to KRAS G12C (PDB ID: 7YCE). **D)** X-ray crystal structure of **ASP6918** bound to KRAS G12C (PDB ID: 8X6R). **E)** X-ray crystal structure of compound **39** bound to KRAS G12D (PDB ID: 7RT4). **F)** X-ray crystal structure of **MRTX1133** bound to KRAS G12D (PDB ID: 7RPZ). Hydrogen bonds are illustrated in yellow and π-π stacking interaction in blue.

3.1.9 Development of other KRAS G12C inhibitors and the second breakthrough in the development of KRAS G12C inhibitors.

Other prominent inhibitors currently in the pipeline and their structural optimization is not yet disclosed are overviewed in this sub-section.

GDC-6036 (Divarasib), developed by Genentech, is a potent and selective KRAS G12C inhibitor, first disclosed at AACR 2022 by Genentech.[96] Like the other approved KRAS G12C inhibitors, **GDC-6036** binds to KRAS in the GDP-bound state. It inhibits KRAS G12C in an HTRF assay with IC_{50} of 2.9 nM and shows greater growth inhibition of KRAS G12C-driven cell lines compared to **Sotorasib** and **Adagrasib**. It shows promising anti-tumor activity in KRAS G12C xenograft models. A phase 1a/1b dose-escalation clinical trial is currently ongoing evaluating the safety and pharmacokinetics (NCT04449874). Initial reports of this trial indicate mostly low-grade adverse events, with grade-3 events in 11% and grade-4 events in only 1% of the patients.[97] A phase 1b clinical trial evaluating GDC-6036 in combination with EGFR inhibitor cituximab reported an objective response rate of 62.5% and median progression-free survival of 8.1 months (NCT04449874).[98]

BI 1823911 is a covalent inhibitor of GDP-bound KRAS G12C developed by Boehringer Ingelheim. While it is known that the compound binds to Switch II pocket and engages Cys12 in a covalent modification, the exact structure remains undisclosed at the time of writing this article. The compound shows potent activity in cellular and in vivo models of KRAS G12C, comparable to **Sotorasib** and **Adagrasib**. A first-in-human phase 1a/b clinical trial (NCT04973163) is ongoing to study the safety, dose-response, and pharmacokinetics. However, of the first 17 patients that received this drug candidate as monotherapy, 8 patients discontinued therapy due to dose-limiting toxicities or disease progression.[86] Further data on this compound is awaited.[99]

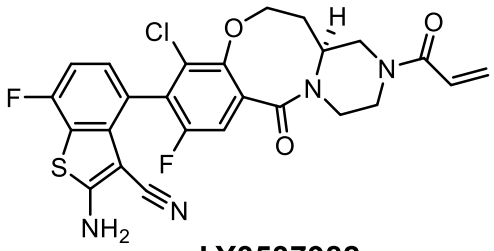

LY3537982

H23 G12C, H358 G12C, and H2122 G12C

IC_{50} = 1.04 x 10^{-3} μM, 1.16 x 10^{-3} μM, and 1.138 x 10^{-2} μM

Figure 15: Chemical structure of **LY3537982**.

LY3537982 (**Olomorasib**) developed by Eli Lilly, is another GDP-bound KRAS G12C inhibitor in clinical development. While the structure of this compound is shown in **Figure 15**, the SAR studies of this compound or its X-ray crystal structure in KRAS G12C have not yet been disclosed. The first disclosure of this potential candidate, presented at AACR 2021,[100] suggested that in a panel of KRAS-driven cell lines, **LY3537982** is selective for KRAS G12C-driven cells. Further, the compound showed significantly better efficacy in various in vitro and vivo models compared to **Sotorasib** and **Adagrasib** and demonstrated synergistic effects when combined with other targeted therapies. A phase 1/2 study evaluating the safety and preliminary efficacy of **LY3537982** is ongoing (NCT04956640). Further, a phase 3 study evaluating the potential of adding **LY3537982** to approved therapies is also underway (NCT04956640 and NCT06119581).

All the KRAS G12C inhibitors described in the above sub-sections bind to the GDP-bound KRAS G12C, which is inactive state. While this approach has advanced scientific understanding and provided therapeutic benefits for the patients, it is noteworthy that oncogenic activity results from the GTP-bound KRAS G12C. Inhibitors of GDP-bound KRAS G12C merely sequester the protein in the inactive state, preventing it from switching to the active state. Developing drug candidates that inhibit the oncogenic form of KRAS G12C remained a challenge until recently.

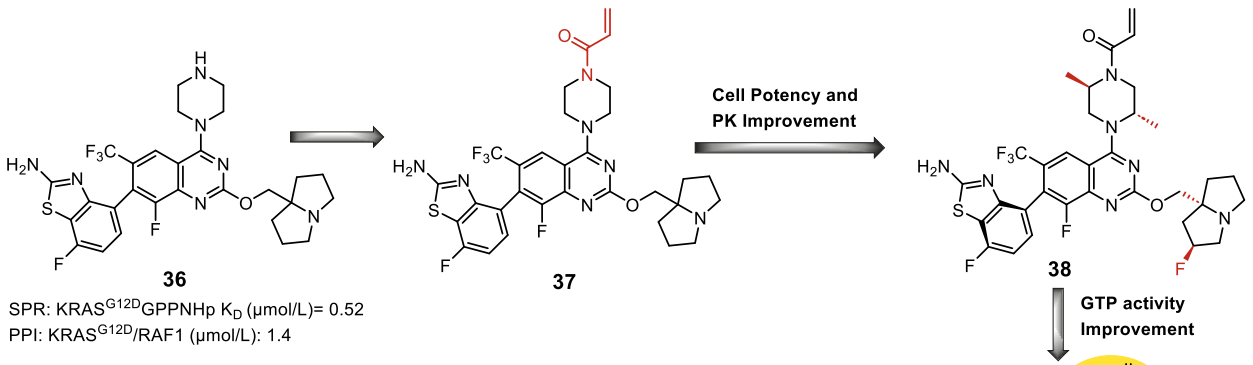

Compounds	MALDI-TOF MS % modification (15 mins)			PPI: KRASG12C/RAF1 (μmol/L)	
	GDP	GppNHp	GTP	GppNHp	GTP
37	80	50	NA	0.14	NA
38	93	97	38	0.12	3.19
BBO-8520	100	100	89	0.026	0.10
Sotorasib	88	0	3	>30	>30
Adagrasib	82	0	1	>30	>30

Figure 16: Optimization of **BBO-8520** through structure-based drug design. **BBO-8520** is a first-in-class covalent dual inhibitor of GTP-Bound and GDP-Bound KRAS G12C.

The second breakthrough in development of KRAS G12C inhibitors was to develop direct and covalent dual inhibitor of GTP-Bound (ON) and GDP-Bound (OFF) KRAS G12C. The BridgeBio Oncology Therapeutics discovered and developed a first-in-class covalent dual inhibitor of GTP-Bound (ON) and GDP-Bound (OFF) KRASG12C, **BBO-8520**, which was disclosed in AACR in 2024 in San Diego.[101] The detailed development of **BBO-8520 is** outlined in **Figure 17.** Initially, they found a measurable noncovalent activity against KRAS G12D (ON) for compound **36** in SPR binding and in a RAF1(RBD) PPI disruption assay.[102] Compound **37** with an acrylamide warhead showed covalent modification of C12 in the (ON) state of KRASG12C, although to a lesser degree than in the (OFF) state. It also showed a limited cellular potency and poor PK properties. Compound **38** was developed by further modification of the quinazoline 2- and 4-position to improve cell potency and ADME properties (clearance and oral bioavailability) of the compound. Although compound **38** showed equal potency against the GDP- and GppNHp-bound proteins in the matrix-assisted laser desorption/ionization-time-of-flight (MALDI-TOF) mass spectrometry-based assay (>90% modification), it lost significant potency when the natural ligand (GTP) was used instead of the nonhydrolyzable analog GppNHp (38% modified). The loss

of potency against the GTP-bound protein was also observed in the PPI assay. They have modified compound 38 to improve GTP activity and further optimization using a structure-based drug design identified BBO-8520, a potent, selective, and direct dual inhibitor of KRASG12C in both (ON) and (OFF) states. **BBO-8520** engaged the target cysteine (C12) rapidly, regardless of nucleotide status, including GTP, as evidenced by MALDI-TOF mass spectrometry measurements. **BBO-8520** also potently disrupted KRASG12C/RAF1(RBD) interaction with an IC_{50} of <100 nmol/L whether KRASG12C was bound to GppNHp or GTP. As expected, both **Sotorasib** and **Adagrasib** showed no activity in this assay. Further, **BBO-8520** showed > 200-fold selectivity over KRAS G12C WT models. A first-in-human Phase 1a/1b clinical trial evaluating the safety, tolerability, and pharmacokinetic properties of **BBO-8520** is ongoing (NCT06343402).

3.2 Direct inhibitors targeting KRAS G12D mutation

KRAS G12D is one of the most frequently occurring mutations in human cancers, with particularly high prevalent in pancreatic ductal adenocarcinoma (PDAC),[103–105] colorectal cancer,[106,107] and non-small cell lung cancer (NSCLC).[108–110] The mutation occurs in approximately 51% of PDAC cases, making it predominant KRAS mutation in this cancer type.[111,112] Despite its prevalence and clinical significance, targeting KRAS G12D has been challenging due to its high affinity for GTP and the absence of suitable binding pockets.[113]

3.2.1 Discovery and development of MRTX1133

Adagrasib (**MRTX849**) a successful KRAS G12C inhibitor developed by Mirati Therapeutics, showed micromolar-range binding affinity with KRAS G12D, indicating a significant scope to enhance G12D potency.[114] Initially, the central bicyclic core of **Adagrasib** was replaced with a pyrido[4,3-d]pyrimidine moiety resulting in compound **39** which showed a K_D = 3.5 μM in the SPR binding affinity assay. The X-ray crystal structure of **39** in KRAS G12D was solved (PDB ID: 7RT4) (**Figure 14E**), and key interactions were identified. The protonated piperazine twist-boat conformation forms a salt bridge with the side chain of Asp12 and its salt bridge with Asp12 are stabilized by an additional hydrogen bond to the carbonyl oxygen of Gly60. The naphthyl substitution at the C7 position occupies a hydrophobic pocket, similar to the binding pose of **Adagrasib**. In the first cycle of SAR studies, the C4 position was optimized by introducing a cyanomethyl (as in **Adagrasib**) or a methyl on the piperazine ring resulted in a

significant loss of activity. Methylation and replacing N with O (affording a morpholine) also attenuated the activity. However, rigidification by introducing bridged bicyclic compounds improved the binding affinity compared to the parent compound (**Figure 17**). Optimization of bridged bicyclic compound at C4 position resulted in a highly potent compound **40**, with HTRF $KRAS^{G12D}$ IC_{50} = 0.005 μM and >200 fold selectivity against WT KRAS. The second SAR cycle involved the optimization of the C2 position. While replacing the pyrrolidinyl group with [6,5] bicyclic systems was not favorable, introducing [5,5] bicyclic systems showed improved activity. Introducing a fluorine at the C3 position of pyrrolizidine as shown in compound **41** improved the cellular activity. The eutomer **41** shows potent pERK cell inhibition with IC_{50} of 24 nM, which is 22-fold better than **40**. In the final SAR cycle, optimization of substitutions on the naphthalene ring was pursued. Substitution at C-8 position of naphthalene ring with smaller moieties like methyl and chloro resulted in 8-30-fold increased potency but showed best results with an alkynyl group. Introducing fluorine on the C7 position and alkynyl on the C8 position at the naphthalene ring, as shown in compound **42**, was equipotent as compound **41** but showed improved PK properties. The hydroxyl group on the C3 of naphthyl showed a 5-fold increased potency than its unsubstituted counterpart. The final compound, **MRTX1133**, was designed by combining the optimized substitutions from the above three SAR cycles optimization and exhibited high affinity for KRAS G12D and potent pERK cellular inhibition (IC_{50} = 2 nM) in AGS cells (**Figure 17**).
X-ray crystal of **MRTX1133** in GDP-bound KRAS G12D was solved to confirm the key interactions (PDB ID: 7RPZ) (**Figure 14F**). All the key interactions optimized during the SAR studies were observed in the crystal structure. N-3 of the central bicycle ring forms a network of water-mediated hydrogen bond interactions with Asp92 and Tyr96, while N-6 nitrogen forms hydrogen bonds with Glu63 and Arg68. The central bicycle ring also forms π-π stacking interaction with Tyr64. The protonated nitrogen of the bridged bicycle forms an electrostatic bond with Asp12. It also forms a network of water-mediated hydrogen bonds. The naphthalene group is buried in a relatively hydrophobic pocket. **MRTX1133** showed potent growth inhibition and demonstrated promising efficacy in xenograft models. The successful preclinical results led to its first-in-human clinical trial (NCT05737706), wherein the drug candidate is evaluated in patients with advanced solid tumors with KRAS G12D mutation.[115]

MRTX1133 binding to KRAS G12D results in moderate stabilization of the protein's dynamic regions, particularly within the Switch II domain. Molecular dynamics simulations[42]

demonstrated that in the inhibitor-free KRAS G12D, residues such as Ala66, Met67, and Arg68 exhibited high flexibility, with RMSF values reaching up to 1.60 Å. Upon binding of MRTX1133, fluctuations in these residues decreased significantly. For example, RMSF for Leu56–Phe78 (Switch II) reduced to 0.71 Å, indicating conformational stabilization. Additionally, inter-residue Cα distances such as Val14-Tyr64 and Val14-Glu62 became more consistent, suggesting that MRTX1133 constrains the nucleotide-binding pocket architecture.

Compared to AMG-510, which covalently binds to KRAS G12C and induces stronger conformational rigidity, MRTX1133, a non-covalent inhibitor, allows more flexibility in the bound state. Torsional analysis further revealed that residues like Thr58 and Pro34 in MRTX1133-bound KRAS G12D still undergo moderate shifts, unlike the more restricted profiles observed with AMG-510. This reflects the relatively less rigid stabilization conferred by non-covalent inhibition.

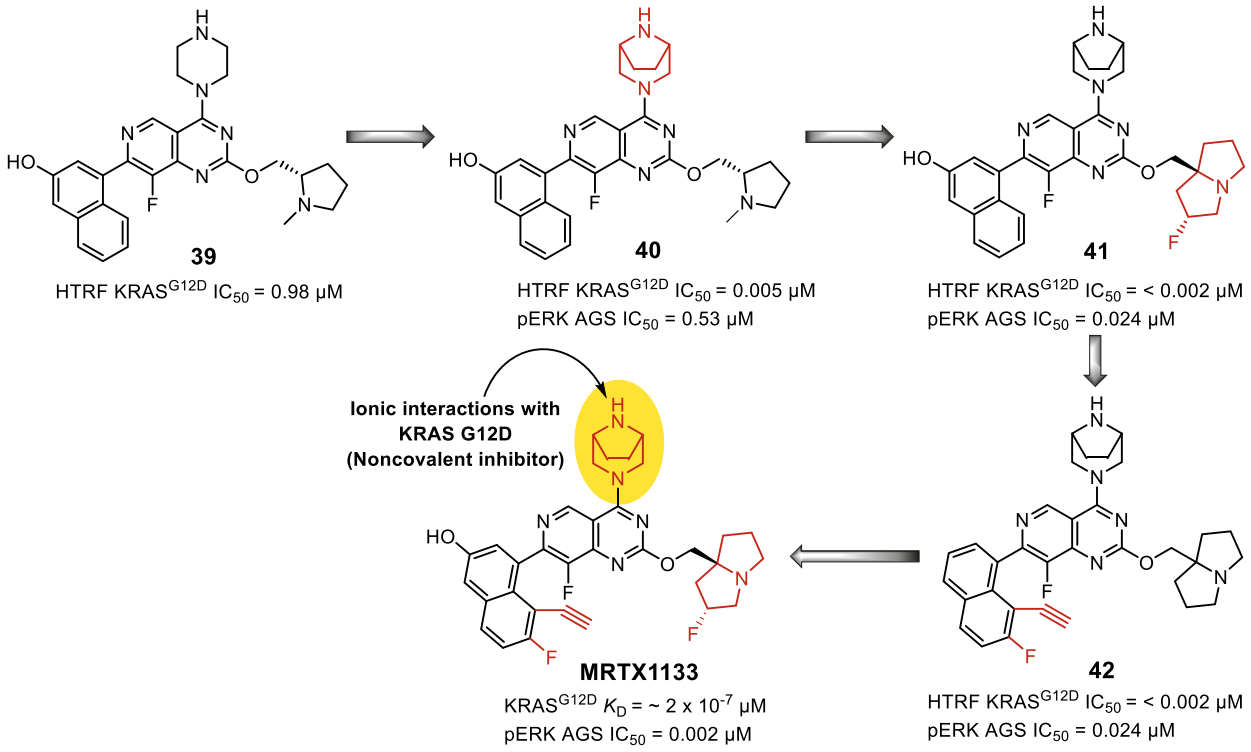

Figure 17: Optimization of **MRTX1133** through structure-based drug design. MRTX1133, one of the early GDP-bound KRAS G12D inhibitors, was developed based on the structural insights gained from identification of MRTS849, a KRAS G12C inhibitor.

3.2.2 Discovery of RMC-9805 (Zoldonrasib)

While the development of **MRTX1133** is a milestone in KRAS G12D-targeted research, a key challenge still needs to be addressed- targeting the oncogenic GTP-bound form of the mutant. This challenge was addressed by the discovery of **RMC-9805**, the first-in-class inhibitor of the GTP-bound KRAS G12D. Revolution Medicines revealed the structure of **RMC-9805** during AACR San Diego 2024.[116] **RMC-9805** is derived from a natural product and its tri-complex molecular glue, which forms a non-covalent ligand-mediated protein-protein interaction between cyclophilin A and GTP-bound RAS. The subsequent covalent modification of the mutant Asp12 residue prevents the target's interaction with RAF and other downstream proteins and affords selectivity over wild-type RAS. In addition to preclinical activity in cellular and xenograft models, **RMC-9805** also demonstrates synergy with other therapies, notably anti-PDL1 therapy. A phase 1a/1b clinical trial is ongoing to evaluating the compound for its safety and tolerability is ongoing (NCT06040541).

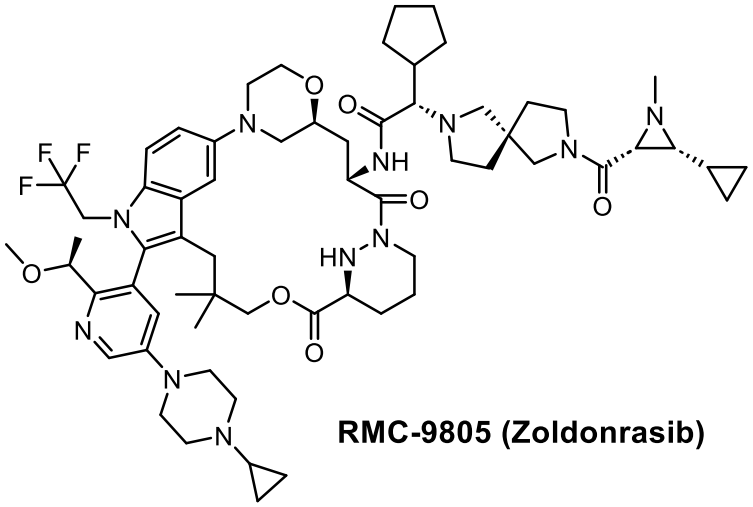

Figure 18: Chemical structure of **RMC-9805 (Zoldonrasib).**

3.2.3 KRAS G12D inhibitors binding to Switch I/II pocket

A 2012 publication by Sun et al reported a compound which directly binds to KRAS between switch I and switch II.[117]Although the binding affinity (K_D = 190 μM) was quite high, this work opened the doors for targeting a new site of KRAS. In the same year, Maurer et al of Genentech reported a fragment,[118] **DCAI**, that binds to the same pocket, albiet with K_D = 1.1 mM.

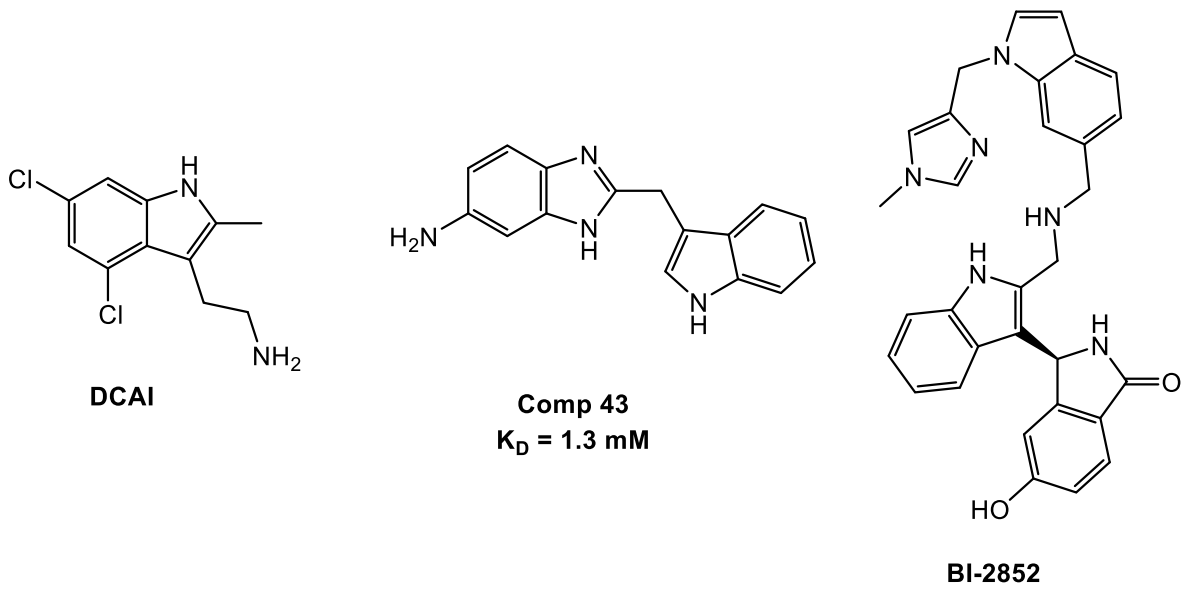

Figure 19: Chemical structures of some Switch I/II pocket inhibitors

While there was no progress in targeting this novel site for next few years, in 2019, Kessler et al from Boehringer Ingelheim reported **BI-2852** with nanomolar affinity and named it the switch I/II pocket.[119] This pocket is shallow and is accessible in both GTP-bound and GDP-bound forms of KRAS. Initially, fragment based screening was performed on in-house libraries to identify a millimolar affinity compound **43**. The indole of **43** forms a hydrogen bond with Asp54. As the pocket is very shallow, the authors aimed to form polar interactions in the pocket with low desolavation costs. Specifically, Thr74 and Glu37 were targeted. A series of SAR optimization studies resulted in the identification of BI-2852. BI-2852 binds non-covalently and targets both the GDP-bound and GTP-bound conformations of KRAS, and shows K_D = 750 nM affinity to GTP-KRAS G12D.

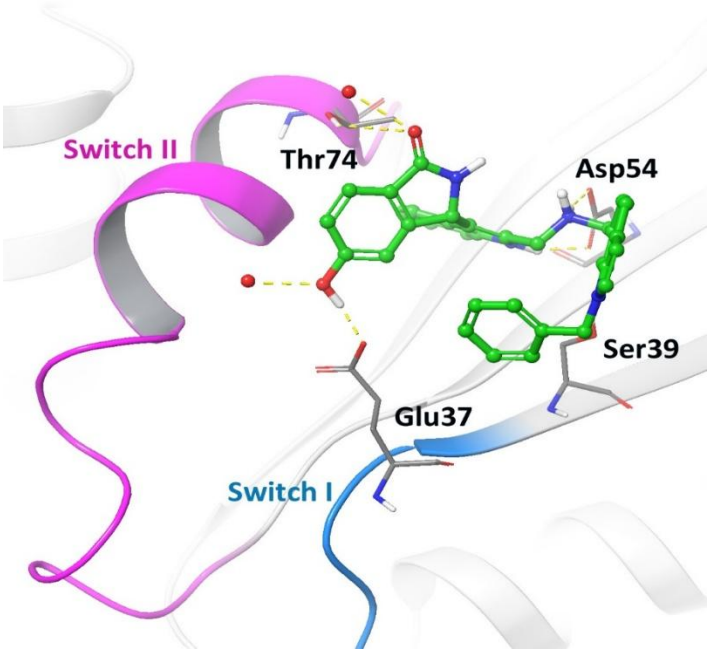

Figure 20: X-ray crystal structure of compound **43** bound to KRAS G12C (PDB ID: 6GJ7). Hydrogen bonds are illustrated in yellow and π-π stacking interaction in blue.

3.3 Direct inhibitors of other KRAS G12 mutants

Beyond G12C[120] and G12D,[121] four additional clinically relevant point mutations occur at codon 12: G12S, G12R, G12V, and G12A.[45,122–125] While these mutations show lower prevalence compared to G12C and G12D, they represent important therapeutic targets. Research targeting these KRAS mutations remains in its early stages, with no clinical studies currently underway.[113,126]

3.3.1 KRAS G12S Inhibitors

The G12S mutation occurs in approximately 5% in both colorectal cancers and non-small cell lung cancer cases, indicating that a successful therapy targeting this mutant could benefit thousands of patients. A 2022 study by Zhang *et al.* demonstrated a novel approach for targeting KRAS G12S through chemical acylation of the acquired serine residue.[127] This strategy was inspired by the known nucleophilic attack by serine and threonine on the highly strained *β*-lactone rings resulting in ring opening. The authors resolved the X-ray crystal structure of GDP-bound KRAS G12S and observed that the structure is very similar to the G12C mutant. Thus, optimization of the **MRTX849** scaffold was used as a strategy. A compound was designed and synthesized,

demonstrating reversible modification and enzyme inhibitory potential. The X-ray crystal structure revealed that 40 binds to KRAS G12S in the switch II pocket, similar to KRAS G12C inhibitors. They also demonstrated reversible modification and enzyme inhibitory potential with compound **43** (**Figure 21**).

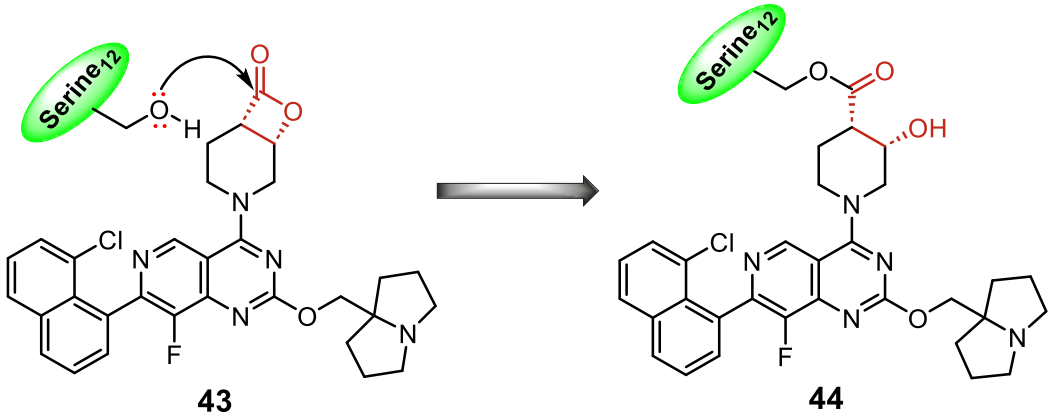

Figure 21: Schematic representation showing a chemical acylation of KRAS serine residue with compound **43**.

3.3.2 KRAS G12R Inhibitors

KRAS G12R represents a particularly challenging target, occurring in approximately 12% of pancreatic ductal adenocarcinoma patients. Recent work has focused on exploiting the unique chemical properties of the arginine side chain. The Shokat laboratory developed a novel approach utilizing the weakly nucleophilic nature of the guanidium moiety of arginine. Their strategy introduced an *α,β*-diketoamide modification of KRAS G12C inhibitor in the Switch II pocket-binding scaffold, resulting in the development of compound **45** that showed selective covalent modification of KRAS G12R, as confirmed by mass spectrometry.[128] Importantly, this compound demonstrated specificity for G12R over other KRAS variants, including G12D, G12V, and wild-type KRAS (**Figure 22**).

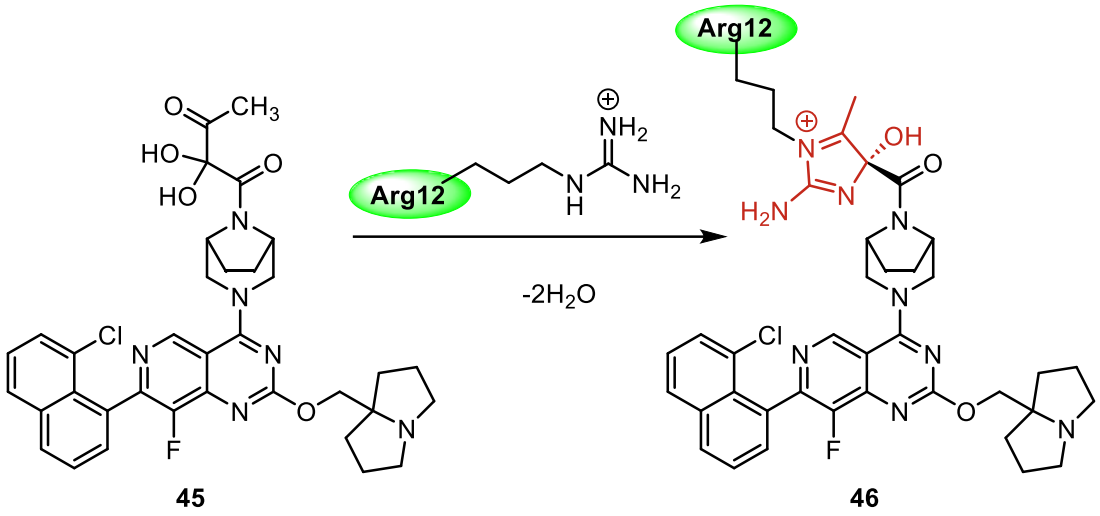

Figure 22: Schematic representation showing an imidazolium condensation product formation between the *α,β*-diketoamide moiety of compound **45** and the ε- and η-nitrogen's of arginine 12.

3.3.3 Targeting challenges for the development of KRAS G12V and G12A inhibitors

While inhibition of KRAS-driven intracellular pathways has historically been challenging, recent studies have identified promising therapeutic approaches. KRAS mutations, particularly G12V, which occurs in 19% of pancreatic, 22% of colon, and 30% of lung adenocarcinomas,[129] have proven difficult to target due to their complex molecular properties. Farnesyl transferase inhibitors (FTIs) such as **Tipifarnib** and **Lonafarnib** have demonstrated antitumor activities against KRAS-mutated cancer cell lines, particularly due to their ability to prevent Ras protein membrane attachment and activation.[130,131] While initial clinical trials with FTIs showed limited efficacy due to dose-limiting toxicities, including myelosuppression and gastrointestinal symptoms, recent studies have demonstrated their potential in combination therapy approaches.[132] Combination therapy with these FTIs produces a synergistic antitumor effect in preclinical models, including those with G12V mutations.[132,133] While FTIs like **FTI-277**, **B956**, **Lonafarnib**, and **Tipifarnib** showed effectiveness in preclinical studies of colon, pancreatic, and lung carcinomas, clinical studies were less promising due to an alternative geranylation pathway that can still facilitate KRAS membrane localization.[129,133] This suggests the possibility of an FTI being clinically relevant beyond HRAS mutant cancers. A significant breakthrough has been achieved with **FGTI-2734**, a novel dual farnesyl and geranylgeranyl transferase inhibitor that specifically prevents KRAS membrane localization and induces apoptosis in mutant KRAS-dependent tumors.[133] This approach directly addresses the alternative geranylation pathway that limited

earlier FTI efficacy. Accordingly, the development of isogenic pancreatic cancer organoid platform provided specific inhibitors to treat mutant KRAS.[129] These platforms have led to the discovery of **Perhexiline maleate**, which uniquely targets KRAS mutations by modulating the cholesterol biosynthesis pathway, as revealed through single-cell RNA-seq analysis.[134] These platforms provide a novel way to test targeted therapies for KRAS mutations, including G12V, that are frequently seen in PDAC.[104,134,135] Recent studies have identified key resistance mechanisms, including the development of Ras inhibitor resistance and alternative pathway activation,[131] as well as activation of RTK-RAS-MAPK and PI3K-AKT-mTOR pathways.[136] Thus, a combination of FTIs and organoid-based platforms may help enrich the therapeutic strategies against KRAS-driven cancers, mainly with G12V and G12A mutations.

4. Resistance mechanisms to direct KRAS inhibitors

KRAS inhibitors targeting the codon 12 oncogenic mutants have shown significant clinical activity, but resistance invariably emerges. In the pivotal CodeBreaK 100 (sotorasib) and KRYSTAL-1 (adagrasib) trials in KRAS G12C-mutant lung cancer, objective response rates ~40% were achieved, yet approximately one-third of patients exhibit primary resistance (progression <3 months) and most others progress within 6–7 months.[137] These outcomes underscore the diverse resistance mechanisms that tumor cells deploy against direct KRAS inhibitors. Intensive studies in both patients and models, including analyses from CodeBreaK/KRYSTAL trials, have identified on-target (drug-specific) and off-target (bypass) resistance pathways across KRAS G12C, G12D, and G12V-driven cancers.

4.1 On-Target (KRAS-Centric) Resistance

Tumors can acquire secondary KRAS mutations that impair inhibitor binding or restore guanine nucleotide exchange. Notably, mutations in the KRAS switch-II pocket (e.g. Y96C/D/S or H95Q/R) disrupt the covalent binding of sotorasib and adagrasib, causing cross-resistance.[138,139] Additional KRAS alterations, such as new activating mutations at G12 (e.g. G12D/V/R) or Q61, or high-level amplification of the KRAS mutant allele, are observed at progression.[140] These changes reactivate RAS signaling despite inhibitor therapy. For example, a patient relapsing on adagrasib was found to harbor an acquired KRAS Y96D mutation that prevented drug binding, alongside polyclonal KRAS/NRAS/BRAF/MAPK1 alterations converging to reactivate the

MAPK pathway.[141] Interestingly, some secondary KRAS mutations confer resistance to one inhibitor but not the other: in vitro screens showed substitutions like A59S, A59T or R68M abrogate sotorasib activity yet remain sensitive to adagrasib, whereas a KRAS Q99L mutation drives adagrasib resistance but retains sotorasib sensitivity.[142] This non-overlapping profile suggests that sequential use of different KRAS G12C inhibitors could overcome certain on-target resistances. Importantly, next-generation KRAS inhibitors are being designed to address these on-target escape mutants. For instance, a novel active-state KRAS^G12C inhibitor has demonstrated inhibition of the resistant KRAS^G12C/Y96D variant in preclinical models.[139]

4.2 Off-Target and Bypass Mechanisms

A majority of resistant cases without new KRAS mutations show activation of compensatory pathways that bypass the need for the inhibited KRAS allele. Upstream receptor tyrosine kinases (RTKs) are frequently implicated. For example, amplification of MET or EGFR can drive persistent signaling through MAPK and PI3K cascades despite KRAS G12C blockade.[142] In KRAS-driven colorectal cancers, feedback EGFR activation has been recognized as a key resistance driver, motivating combinatorial therapy (e.g. adagrasib plus the anti-EGFR antibody cetuximab in KRYSTAL-1) to achieve deeper and more durable responses.[143] Downstream pathway reactivation via parallel oncogenic mutations is another recurrent theme. Resistant tumors have been found to harbor new activating mutations in NRAS or HRAS, BRAF^V600E or MAP2K1 (MEK1), and even gene fusions involving ALK, RET, RAF1, BRAF, or FGFR3 – all events that resurrect the ERK signaling flux independent of KRAS G12C.[144] Loss-of-function alterations in tumor suppressors that normally constrain proliferative signaling, such as NF1 (a RAS GTPase-activating protein) or PTEN (a PI3K pathway inhibitor), are also documented mechanisms that relieve negative regulation and sustain growth signals under KRAS inhibitor pressure.[145] In pancreatic ductal adenocarcinoma (a KRAS^G12D-driven setting), resistant tumors emerging on KRAS inhibitors frequently exhibit activation of the PI3K–AKT–mTOR axis [146]or cell-cycle accelerators; for instance, emergent PIK3CA mutations and amplifications of MYC, CDK6, or KRAS itself have been observed at relapse. These diverse bypass alterations often co-occur within the same tumor (polyclonal resistance), all funneling into reactivation of downstream proliferative pathways. Co-occurring genomic context can further modulate resistance: common co-mutations in KRAS-mutant lung adenocarcinomas (such as in STK11/LKB1 or KEAP1) are

associated with distinct biologic behavior and may confer a predisposition to certain resistance routes or affect therapeutic responsiveness.[147,148]

4.3 Phenotypic transformation resulting in resistance

Beyond genetic alterations, tumors often employ phenotypic transformation and adaptive signaling rewiring as resistance strategies against direct KRAS inhibition. Clinical analyses have demonstrated that KRAS^G12C-mutant non-small cell lung cancers (NSCLC) treated with adagrasib can undergo histological transformations, such as from adenocarcinoma to squamous cell carcinoma, without acquiring identifiable secondary mutations. This phenotypic shift enables cancer cells to evade dependency on initial lineage-specific signaling and survive KRAS inhibition by adopting alternate differentiation states, analogous to lineage plasticity observed during resistance to EGFR inhibitors.[149]

For deeper understanding of resistance mechanisms to KRAS inhibitors, the interested reader is directed to several good reviews on this matter.[150-152]

5. Conclusion and future perspective

Over the past decade, the landscape of KRAS-targeted drug discovery has undergone a remarkable transformation. Once deemed undruggable due to its picomolar GTP affinity and lack of accessible binding pockets, KRAS, particularly with codon 12 mutations, has now become a viable therapeutic target, driven by innovations in structure-guided drug design. The breakthrough identification of the Switch-II pocket by the Shokat lab enabled the rational development of covalent inhibitors selectively targeting KRAS G12C, culminating in the FDA approval of sotorasib and adagrasib. These agents have demonstrated clinical efficacy, particularly in NSCLC, and represent a significant milestone in precision oncology.

Subsequent design efforts have expanded to other G12 mutants such as G12D, G12R, and G12S. However, many of these are still in clinical development and awaiting regulatory approval. Dual inhibitors targeting both GDP- and GTP-bound KRAS G12C, such as BBO-8520, address limitations of earlier compounds and offer expanded therapeutic windows. Simultaneously, emerging approaches, including GDP mimetics, allosteric binders, and tri-complex molecular glues, provide alternative avenues for disrupting KRAS activity, even in mutants lacking reactive residues.

Despite the clinical success of KRAS G12C inhibitors such as sotorasib and adagrasib, the emergence of acquired resistance remains a major therapeutic challenge. Resistance mechanisms are multifaceted and may include secondary mutations in KRAS that impair inhibitor binding (e.g., Y96D, H95Q/R), upregulation of bypass signaling pathways such as EGFR, MET, or PI3K, and adaptive feedback activation of upstream receptor tyrosine kinases. Additionally, nucleotide cycling from the GDP-bound to the GTP-bound state can diminish the efficacy of inhibitors that target only the inactive conformation. Some tumors also exhibit KRAS-independent survival mechanisms, where cells become less reliant on KRAS signaling through reprogramming of survival pathways or lineage plasticity. Combination strategies, such as co-targeting SH2-domain containing proteins, RTKs, mTOR, or components of the cell cycle machinery, are being actively explored to overcome these limitations. A deeper understanding of resistance biology is essential to guide the rational design of next-generation KRAS inhibitors and combination regimens.

In summary, the evolution of structure-based design strategies has transformed KRAS from an intractable target into a druggable oncogene, and holds promise for expanding therapeutic options for patients harboring KRAS-driven malignancies.

ACKNOWLEDGEMENTS

The research work in Gavande laboratory is supported by the National Institutes of Health (R01CA247370 and R01AI161570), the Department of Defense (W81XWH-22-1-0369), the VA, KCI's Michigan SPORE, Richard Barber Interdisciplinary Research Program, DMC Foundation, WSU Applebaum Faculty Research Award (FRAP) and the Wayne State University. Sadaf Dorandish and Jeremy Kelm are supported by the NIH funded Wayne State University Chemistry Biology Interface (CBI) Program T32GM142519-01.

The research work in Lakkaniga laboratory is supported by the Science and Engineering Research Board (SERB), Government of India, Grant no. SRG/2022/000091.

CONFLICT OF INTEREST STATEMENT

The authors declare no conflict of interest. All authors contributed essential portions of the manuscript, reviewed, and approved the final manuscript.

DATA AVAILABILITY STATEMENT

Data sharing is not applicable to this article as no data has been generated or analyzed in this paper.

References:

1. Uprety D, Adjei AA. KRAS: From undruggable to a druggable Cancer Target. *Cancer Treat Rev*. 2020;89:102070.

2. Eser S, Schnieke A, Schneider G, Saur D. Oncogenic KRAS signalling in pancreatic cancer. *British Journal of Cancer*. 2014;111(5):817-822.

3. Buscail L, Bournet B, Cordelier P. Role of oncogenic KRAS in the diagnosis, prognosis and treatment of pancreatic cancer. *Nature Reviews Gastroenterology & Hepatology*. 2020;17(3):153-168.

4. Ferrer I, Zugazagoitia J, Herbertz S, John W, Paz-Ares L, Schmid-Bindert G. KRAS-Mutant non-small cell lung cancer: From biology to therapy. *Lung Cancer*. 2018;124:53-64.

5. Aviel-Ronen S, Blackhall FH, Shepherd FA, Tsao MS. K-ras Mutations in Non-Small-Cell Lung Carcinoma: A Review. *Clin Lung Cancer*. 2006;8(1):30-38.

6. Zhu G, Pei L, Xia H, Tang Q, Bi F. Role of oncogenic KRAS in the prognosis, diagnosis and treatment of colorectal cancer. *Molecular Cancer 2021 20:1*. 2021;20(1):1-17.

7. Huang L, Guo Z, Wang F, Fu L. KRAS mutation: from undruggable to druggable in cancer. *Signal Transduct Target Ther*. 2021;6(1):386.

8. Stolze B, Reinhart S, Bulllinger L, Fröhling S, Scholl C. Comparative analysis of KRAS codon 12, 13, 18, 61 and 117 mutations using human MCF10A isogenic cell lines. *Scientific Reports* 2015;5(1):1-9.

9. Santarpia L, Lippman SM, El-Naggar AK. Targeting the MAPK–RAS–RAF signaling pathway in cancer therapy. *Expert Opin Ther Targets*. 2012;16(1):103-119.

10. Simanshu DK, Nissley D V., McCormick F. RAS Proteins and Their Regulators in Human Disease. *Cell*. 2017;170(1):17-33.

11. Wee S, Jagani Z, Kay XX, et al. PI3K pathway activation mediates resistance to MEK inhibitors in KRAS mutant cancers. *Cancer Res*. 2009;69(10):4286-4293.

12. Yoshizawa A, Sumiyoshi S, Sonobe M, Kobayashi M, Fujimoto M, Kawakami F, Tsuruyama T, Travis W.D, Date H, Haga H. Validation of the IASLC/ATS/ERS lung adenocarcinoma classification for prognosis and association with EGFR and KRAS gene mutations: analysis of 440 Japanese patients. *Journal of Thoracic Oncology.* 2013;8(1):52-61.

13. Dearden S, Stevens J, Wu YL, Blowers D. Mutation incidence and coincidence in non-small-cell lung cancer: Meta-analyses by ethnicity and histology (mutMap). *Annals of Oncology*. 2013;24(9):2371-2376.

14. Shepherd FA, Domerg C, Hainaut P, et al. Pooled analysis of the prognostic and predictive effects of KRAS mutation status and KRAS mutation subtype in early-stage resected non-small-cell lung cancer in four trials of adjuvant chemotherapy. *Journal of Clinical Oncology*. 2013;31(17):2173-2181.

15. El Osta B, Behera M, Kim S, et al. Characteristics and Outcomes of Patients With Metastatic KRAS-Mutant Lung Adenocarcinomas: The Lung Cancer Mutation Consortium Experience. *Journal of Thoracic Oncology*. 2019;14(5):876-889.

16. Dogan S, Shen R, Ang DC, et al. Molecular epidemiology of EGFR and KRAS mutations in 3,026 lung adenocarcinomas: Higher susceptibility of women to smoking-related KRAS-mutant cancers. *Clinical Cancer Research*. 2012;18(22):6169-6177.

17. Dienstmann R, Connor K, Byrne AT, Fridman WH, Lambrechts D, Sadanandam A, Trusolino L, Prehn JHM, Tabernero J, Kolch W. Precision therapy in RAS mutant colorectal cancer. *Gastroenterology*. 2020;158(4),806-811.

18. Bray F, Ferlay J, Soerjomataram I, Siegel RL, Torre LA, Jemal A. Global cancer statistics 2018: GLOBOCAN estimates of incidence and mortality worldwide for 36 cancers in 185 countries. *CA Cancer J Clin*. 2018;68(6):394-424.

19. Dienstmann R, Mason MJ, Sinicrope FA, et al. Prediction of overall survival in stage II and III colon cancer beyond TNM system: a retrospective, pooled biomarker study. *Ann Oncol*. 2017;28(5):1023-1031.

20. Amado RG, Wolf M, Peeters M, et al. Wild-type KRAS is required for panitumumab efficacy in patients with metastatic colorectal cancer. *J Clin Oncol*. 2008;26(10):1626-1634.

21. Park W, Chawla A, O'Reilly EM. Pancreatic Cancer: A Review. *JAMA - Journal of the American Medical Association*. 2021;326(9):851-862.

22. Gasper R, Wittinghofer F. The Ras switch in structural and historical perspective. *Biol Chem*. 2020;401(1):143-163.

23. Nussinov R, Tsai CJ, Jang H. Independent and core pathways in oncogenic KRAS signaling. *Expert Rev Proteomics*. 2016;13(8):711-716.

24. Tape CJ, Ling S, Dimitriadi M, et al. Oncogenic KRAS Regulates Tumor Cell Signaling via Stromal Reciprocation. *Cell*. 2016;165(4):910-920.

25. Crespo P, León J. Ras proteins in the control of the cell cycle and cell differentiation. *Cellular and Molecular Life Sciences*. 2000;57(11):1613-1636.

26. Haigis KM, Kendall KR, Wang Y, et al. Differential effects of oncogenic K-Ras and N-Ras on proliferation, differentiation and tumor progression in the colon. *Nature Genetics*. 2008;40(5):600-608.

27. Parikh C, Subrahmanyam R, Ren R. Oncogenic NRAS, KRAS, and HRAS Exhibit Different Leukemogenic Potentials in Mice. *Cancer Res*. 2007;67(15):7139-7146.

28. Janakiraman M, Vakiani E, Zeng Z, et al. Genomic and biological characterization of exon 4 KRAS mutations in human cancer. *Cancer Res*. 2010;70(14):5901-5911.

29. Whitley MJ, Tran TH, Rigby M, et al. Comparative analysis of KRAS4a and KRAS4b splice variants reveals distinctive structural and functional properties. *Sci Adv*. 2024;10(7).

30. Ahearn IM, Haigis K, Bar-Sagi D, Philips MR. Regulating the regulator: post-translational modification of RAS. *Nat Rev Mol Cell Biol*. 2011;13(1):39-51.

31. Pandey D, Chauhan SC, Kashyap VK, Roy KK. Structural insights into small-molecule KRAS inhibitors for targeting KRAS mutant cancers. *Eur J Med Chem*. 2024;277.

32. Boguski MS, McCormick F. Proteins regulating Ras and its relatives. *Nature*. 1993;366(6456):643-654.

33. Wang W hua, Yuan T, Qian M jia, et al. Post-translational modification of KRAS: potential targets for cancer therapy. *Acta Pharmacologica Sinica.* 2020;42(8):1201-1211.

34. Wright LP, Philips MR. Thematic review series: lipid posttranslational modifications. CAAX modification and membrane targeting of Ras. *J Lipid Res*. 2006;47(5):883-891.

35. Nuevo-Tapioles C, Philips MR. The role of KRAS splice variants in cancer biology. *Front Cell Dev Biol*. 2022;10:1033348-1033348.

36. Zhao H, Liu P, Zhang R, et al. Roles of palmitoylation and the KIKK membrane-targeting motif in leukemogenesis by oncogenic KRAS4A. *J Hematol Oncol*. 2015;8(1):1-14.

37. Tsai FD, Lopes MS, Zhou M, et al. K-Ras4A splice variant is widely expressed in cancer and uses a hybrid membrane-targeting motif. *Proc Natl Acad Sci U S A*. 2015;112(3):779-784.

38. Kattan WE, Hancock JF. RAS Function in cancer cells: translating membrane biology and biochemistry into new therapeutics. *Biochem J*. 2020;477(15):2893-2919.

39. Hofer F, Fields S, Schneider C, Martin GS. Activated Ras interacts with the Ral guanine nucleotide dissociation stimulator. *Proc Natl Acad Sci U S A*. 1994;91(23):11089-11093.

40. Wood KW, Sarnecki C, Roberts TM, Blenis J. ras mediates nerve growth factor receptor modulation of three signal-transducing protein kinases: MAP kinase, Raf-1, and RSK. *Cell*. 1992;68(6):1041-1050.

41. Hajdúch M, Jančík S, Drábek J, Radzioch D. Clinical relevance of KRAS in human cancers. *J Biomed Biotechnol*. 2010;(1):150960.

42. Pandey D, Roy KK. Decoding KRAS dynamics: Exploring the impact of mutations and inhibitor binding. *Arch Biochem Biophys*. 2025;764:110279.

43. Lu S, Jang H, Muratcioglu S, et al. Ras Conformational Ensembles, Allostery, and Signaling. *Chem Rev*. 2016;116(11):6607-6665.

44. Yang MH, Tran TH, Hunt B, et al. Allosteric Regulation of Switch-II Domain Controls KRAS Oncogenicity. *Cancer Res*. 2023;83(19):3176-3183.

45. Hunter JC, Manandhar A, Carrasco MA, Gurbani D, Gondi S, Westover KD. Biochemical and structural analysis of common cancer-associated KRAS mutations. *Molecular Cancer Research*. 2015;13(9):1325-1335.

46. Boriack-Sjodin PA, Margarit SM, Bar-Sagi D, Kuriyan J. The structural basis of the activation of Ras by Sos. *Nature*. 1998;394(6691):337-343.

47. Pai EF, Kabsch W, Krengel U, Holmes KC, John J, Wittinghofer A. Structure of the guanine-nucleotide-binding domain of the Ha-ras oncogene product p21 in the triphosphate conformation. *Nature*. 1989;341(6239):209-214.

48. Overbeck AF, Brtva TR, Cox AD, et al. Guanine nucleotide exchange factors: Activators of Ras superfamily proteins. *Mol Reprod Dev*. 1995;42(4):468-476.

49. Ferreira A, Pereira F, Reis C, Oliveira MJ, Sousa MJ, Preto A. Crucial Role of Oncogenic KRAS Mutations in Apoptosis and Autophagy Regulation: Therapeutic Implications. *Cells*. 2022;11(14): 2183.

50. Moghadamchargari Z, Shirzadeh M, Liu C, et al. Molecular assemblies of the catalytic domain of SOS with KRas and oncogenic mutants. *Proc Natl Acad Sci U S A*. 2021;118(12):e2022403118.

51. Lu S, Jang H, Zhang J, Nussinov R. Inhibitors of Ras–SOS Interactions. *ChemMedChem*. 2016;11(8):814-821.

52. Hancock JF. Ras proteins: different signals from different locations. *Nat Rev Mol Cell Biol*. 2003;4(5):373-384.

53. Prior IA, Hood FE, Hartley JL. The Frequency of Ras Mutations in Cancer. *Cancer Res*. 2020;80(14):2669-2974.

54. Knobbe CB, Reifenberger J, Reifenberger G. Mutation analysis of the Ras pathway genes NRAS, HRAS, KRAS and BRAF in glioblastomas. *Acta Neuropathol*. 2004;108(6):467-470.

55. Bar-Sagi D. A Ras by any other name. *Mol Cell Biol*. 2001;21(5):1441-1443.

56. Prior IA, Lewis PD, Mattos C. A Comprehensive Survey of Ras Mutations in Cancer. *Cancer Res*. 2012;72(10):2457-2467.

57. Dharmaiah S, Bindu L, Tran TH, et al. Structural basis of recognition of farnesylated and methylated KRAS4b by PDEd. *Proc Natl Acad Sci U S A*. 2016;113(44): E6766-E6775.

58. Gregory MC, McLean MA, Sligar SG. Interaction of KRas4b with Anionic Membranes: A Special Role for PIP2. *Biochem Biophys Res Commun*. 2017;487(2):351.

59. Chiosea SI, Miller M, Seethala RR. HRAS Mutations in Epithelial–Myoepithelial Carcinoma. *Head Neck Pathol*. 2014;8(2):146-150.

60. Ney GM, Yang KB, Ng V, et al. Oncogenic N-ras mitigates oxidative stress–induced apoptosis of hematopoietic stem cells. *Cancer Res*. 2021;81(5):1240-1251.

61. Muñoz-Maldonado C, Zimmer Y, Medová M. A comparative analysis of individual ras mutations in cancer biology. *Front Oncol*. 2019;9:492285.

62. Miller MS, Miller LD. RAS mutations and oncogenesis: Not all RAS mutations are created equally. *Front Genet*. 2012;2:15127.

63. Ho AL, Brana I, Haddad R, et al. Tipifarnib in head and neck squamous cell carcinoma with HRAS mutations. *Journal of Clinical Oncology*. 2021;39(17):1856-1864.

64. Sasaki E, Masago K, Fujita S, Hanai N, Yatabe Y. Frequent KRAS and HRAS mutations in squamous cell papillomas of the head and neck. *J Pathol Clin Res*. 2020;6(2):154-159.

65. Sugita S, Enokida H, Yoshino H, Miyamoto K, Yonemori M, Sakaguchi T, Osako Y, Nakagawa M. HRAS as a potential therapeutic target of salirasib RAS inhibitor in bladder cancer. *International Journal of Oncology*. 2018;53(2):725-736.

66. Dou R, Zhang L, Lu T, Liu D, Mei F, Huang J, Qian L. Identification of a novel HRAS variant and its association with papillary thyroid carcinoma. *Oncology letters*. 2018;15(4):4511-4516.

67. Lakkaniga NR, Wang Z, Xiao Y, Kharbanda A, Lan L, Li H yu. Revisiting Aurora Kinase B: A promising therapeutic target for cancer therapy. *Med Res Rev*. 2024;44(2):686-706.

68. Halder P, Rai A, Talukdar V, Das P, Lakkaniga NR. Pyrazolopyridine-based kinase inhibitors for anti-cancer targeted therapy. *RSC Med Chem*. 2024;15(5):1452-1470.

69. Acharya B, Saha D, Armstrong D, Lakkaniga NR, Frett B. FLT3 inhibitors for acute myeloid leukemia: successes, defeats, and emerging paradigms. *RSC Med Chem*. 2022;13(7):798-816.

70. Yan W, Lakkaniga NR, Carlomagno F, et al. Insights into Current Tropomyosin Receptor Kinase (TRK) Inhibitors: Development and Clinical Application. *J Med Chem*. 2019;62(4):1731-1760.

71. Berrozpe G, Schaeffer J, Peinado MA, Real FX, Perucho M. Comparative analysis of mutations in the p53 and K-ras genes in pancreatic cancer. *Int J Cancer*. 1994;58(2):185-191.

72. Ostrem JM, Peters U, Sos ML, Wells JA, Shokat KM. K-Ras(G12C) inhibitors allosterically control GTP affinity and effector interactions. *Nature*. 2013;503(7477):548-551.

73. Patricelli MP, Janes MR, Li LS, et al. Selective inhibition of oncogenic KRAS output with small molecules targeting the inactive state. *Cancer Discov*. 2016;6(3):316-329.

74. Janes MR, Zhang J, Li LS, et al. Targeting KRAS Mutant Cancers with a Covalent G12C-Specific Inhibitor. *Cell*. 2018;172(3):578-589.

75. Shin Y, Jeong JW, Wurz RP, et al. Discovery of N-(1-Acryloylazetidin-3-yl)-2-(1 H-indol-1-yl)acetamides as Covalent Inhibitors of KRASG12C. *ACS Med Chem Lett*. 2019;10(9):1302-1308.

76. Lanman BA, Allen JR, Allen JG, et al. Discovery of a Covalent Inhibitor of KRASG12C (AMG 510) for the Treatment of Solid Tumors. *J Med Chem*. 2020;63(1):52-65.

77. Kettle JG, Cassar DJ. Covalent inhibitors of the GTPase KRASG12C: a review of the patent literature. *Expert Opin Ther Pat*. 2020;30(2):103-120.

78. Ostrem JML, Shokat KM. Targeting KRAS G12C with Covalent Inhibitors. *Annu Rev Cancer Biol*. 2022;6:49-64.

79. Canon J, Rex K, Saiki AY, et al. The clinical KRAS(G12C) inhibitor AMG 510 drives anti-tumour immunity. *Nature*. 2019;575(7781):217-223.

80. Skoulidis F, Li BT, Dy GK, et al. Sotorasib for Lung Cancers with KRAS p.G12C Mutation. *N Engl J Med*. 2021;384(25):2371-2381.

81. Fell JB, Fischer JP, Baer BR, et al. Discovery of Tetrahydropyridopyrimidines as Irreversible Covalent Inhibitors of KRAS-G12C with in Vivo Activity. *ACS Med Chem Lett*. 2018;9(12):1230-1234.

82. Fell JB, Fischer JP, Baer BR, et al. Identification of the Clinical Development Candidate MRTX849, a Covalent KRASG12C Inhibitor for the Treatment of Cancer. *J Med Chem*. 2020;63(13):6679-6693.

83. Hansen R, Peters U, Babbar A, et al. The reactivity-driven biochemical mechanism of covalent KRASG12C inhibitors. *Nat Struct Mol Biol*. 2018;25(6):454-462.

84. Pantsar T. The current understanding of KRAS protein structure and dynamics. *Comput Struct Biotechnol J*. 2020;18:189-198.

85. Hallin J, Engstrom LD, Hargi L, et al. The KRASG12C Inhibitor MRTX849 Provides Insight toward Therapeutic Susceptibility of KRAS-Mutant Cancers in Mouse Models and Patients. *Cancer Discov*. 2020;10(1):54-71.

86. Khan HY, Nagasaka M, Li Y, et al. Inhibitor of the Nuclear Transport Protein XPO1 Enhances the Anticancer Efficacy of KRAS G12C Inhibitors in Preclinical Models of KRAS G12C–Mutant Cancers. *Cancer Research Communications*. 2022;2(5):342-352.

87. Christensen JG, Olson P, Briere T, Wiel C, Bergo MO. Targeting Krasg12c-mutant cancer with a mutation-specific inhibitor. *J Intern Med*. 2020;288(2):183-191.

88. Yaeger R, Uboha N V., Pelster MS, et al. Efficacy and Safety of Adagrasib plus Cetuximab in Patients with KRASG12C-Mutated Metastatic Colorectal Cancer. *Cancer Discov*. 2024;14(6):982-993.

89. Mahran R, Kapp JN, Valtonen S, et al. Beyond KRAS(G12C): Biochemical and Computational Characterization of Sotorasib and Adagrasib Binding Specificity and the Critical Role of H95 and Y96. *ACS Chem Biol*. 2024;19(10):2152-2164.

90. Rubinson DA, Tanaka N, de la Cruz FF, et al. Sotorasib Is a Pan-RASG12C Inhibitor Capable of Driving Clinical Response in NRASG12C Cancers. *Cancer Discov*. 2024;14(5):727-736.

91. Lorthiois E, Gerspacher M, Beyer KS, et al. JDQ443, a Structurally Novel, Pyrazole-Based, Covalent Inhibitor of KRASG12Cfor the Treatment of Solid Tumors. *J Med Chem*. 2022;65(24):16173-16203.

92. Xiong Y, Lu J, Hunter J, et al. Covalent guanosine mimetic inhibitors of G12C KRAS. *ACS Med Chem Lett*. 2017;8(1):61-66.

93. Lim SM, Westover KD, Ficarro SB, et al. Therapeutic targeting of oncogenic K-Ras by a covalent catalytic site inhibitor. *Angew Chem Int Ed Engl*. 2014;53(1):199-204.

94. Imaizumi T, Akaiwa M, Abe T, et al. Discovery and biological evaluation of 1-{2,7-diazaspiro[3.5]nonan-2-yl}prop-2-en-1-one derivatives as covalent inhibitors of KRAS G12C with favorable metabolic stability and anti-tumor activity. *Bioorg Med Chem*. 2022;71.

95. Imaizumi T, Shimada I, Satake Y, et al. Discovery of ASP6918, a KRAS G12C inhibitor: Synthesis and structure–activity relationships of 1-{2,7-diazaspiro[3.5]non-2-yl}prop-2-en-1-one derivatives as covalent inhibitors with good potency and oral activity for the treatment of solid tumors. *Bioorg Med Chem*. 2024;98:117581.

96. Xu J, Lim NK, Timmerman JC, et al. Second-Generation Atroposelective Synthesis of KRAS G12C Covalent Inhibitor GDC-6036. *Org Lett*. 2023;25(19):3417-3422.

97. Sacher, A., LoRusso, P., Patel, M. R., Miller Jr, W. H., Garralda, E., Forster, M. D., ... & Desai, J. Single-agent divarasib (GDC-6036) in solid tumors with a KRAS G12C mutation. *NEW ENGL J MED*. 2023;*389*(8):710-721.

98. Desai J, Alonso G, Kim SH, et al. Divarasib plus cetuximab in KRAS G12C-positive colorectal cancer: a phase 1b trial. *Nat Med*. 2024;30(1):271-278.

99. Xie X, Yu T, Li X, et al. Recent advances in targeting the "undruggable" proteins: from drug discovery to clinical trials. *Signal Transduction and Targeted Therapy.* 2023;8(1):1-71.

100. Peng SB, Si C, Zhang Y, et al. Abstract 1259: Preclinical characterization of LY3537982, a novel, highly selective and potent KRAS-G12C inhibitor. *Cancer Res*. 2021;81(13_Supplement):1259-1259.

101. Caughey BA, Strickler JH. Targeting KRAS-Mutated Gastrointestinal Malignancies with Small-Molecule Inhibitors: A New Generation of Breakthrough Therapies. *Drugs*. 2024;84(1):27-44.

102. Maciag, A. E., Stice, J. P., Wang, B., Sharma, A. K., Chan, A. H., Lin, K., ... & Beltran, P. J. (2025). Discovery of BBO-8520, a first-in-class direct and covalent dual inhibitor of GTP-bound (ON) and GDP-bound (OFF) KRASG12C. *Cancer Discovery*, OF1-OF17.

103. Shen H, Lundy J, Strickland AH, et al. KRAS G12D Mutation Subtype in Pancreatic Ductal Adenocarcinoma: Does It Influence Prognosis or Stage of Disease at Presentation? *Cells*. 2022;11(19):3175.

104. Bournet B, Muscari F, Buscail C, et al. KRAS G12D mutation subtype is a prognostic factor for advanced pancreatic adenocarcinoma. *Clin Transl Gastroenterol*. 2016;7(3):E157.

105. Gu M, Gao Y, Chang P. KRAS Mutation Dictates the Cancer Immune Environment in Pancreatic Ductal Adenocarcinoma and Other Adenocarcinomas. *Cancers*. 2021;13(10):2429.

106. Olmedillas-López S, Lévano-Linares DC, Alexandre CLA, et al. Detection of KRAS G12D in colorectal cancer stool by droplet digital PCR. *World J Gastroenterol*. 2017;23(39):7087.

107. Koulouridi A, Karagianni M, Messaritakis I, et al. Prognostic Value of KRAS Mutations in Colorectal Cancer Patients. *Cancers (Basel)*. 2022;14(14):3320.

108. Ricciuti B, Alessi J V., Elkrief A, et al. Dissecting the clinicopathologic, genomic, and immunophenotypic correlates of KRASG12D-mutated non-small-cell lung cancer. *Annals of Oncology*. 2022;33(10):1029-1040.

109. Liu C, Zheng S, Wang Z, et al. KRAS-G12D mutation drives immune suppression and the primary resistance of anti-PD-1/PD-L1 immunotherapy in non-small cell lung cancer. *Cancer Commun*. 2022;42(9):828-847.

110. Lei L, Wang W xian, Yu Z yang, et al. A Real-World Study in Advanced Non–Small Cell Lung Cancer with KRAS Mutations. *Transl Oncol*. 2020;13(2):329-335.

111. Löhr M, Klöppel G, Maisonneuve P, Lowenfels AB, Lüttges J. Frequency of K-ras Mutations in Pancreatic Intraductal Neoplasias Associated with Pancreatic Ductal Adenocarcinoma and Chronic Pancreatitis: A Meta-Analysis. *Neoplasia*. 2005;7(1):17-23.

112. Zeitouni D, Pylayeva-Gupta Y, Der CJ, Bryant KL. KRAS Mutant Pancreatic Cancer: No Lone Path to an Effective Treatment. *Cancers*. 2016;8(4):45.

113. Zeissig MN, Ashwood LM, Kondrashova O, Sutherland KD. Next batter up! Targeting cancers with KRAS-G12D mutations. *Trends Cancer*. 2023;9(11):955-967.

114. Wang X, Allen S, Blake JF, et al. Identification of MRTX1133, a Noncovalent, Potent, and Selective KRASG12DInhibitor. *J Med Chem*. 2022;65(4):3123-3133.

115. Wei D, Wang L, Zuo X, Maitra A, Bresalier RS. A small molecule with big impact: MRTX1133 targets the KRASG12D mutation in pancreatic cancer. *Clin Cancer Res*. 2024;30(4):655.

116. Knox JE, Burnett GL, Weller C, et al. Abstract ND03: Discovery of RMC-9805, an oral, covalent tri-complex KRASG12D(ON) inhibitor. *Cancer Res*. 2024;84(7_Supplement):ND03-ND03.

117. Sun Q, Burke JP, Phan J, et al. Discovery of Small Molecules that Bind to K-Ras and Inhibit Sos-Mediated Activation. *Angewandte Chemie International Edition*. 2012;51(25):6140-6143.

118. Maurer, T., Garrenton, L. S., Oh, A., Pitts, K., Anderson, D. J., Skelton, N. J., ... & Fang, G. Small-molecule ligands bind to a distinct pocket in Ras and inhibit SOS-mediated nucleotide exchange activity. *Proceedings of the National Academy of Sciences*. 2012;109(14):5299-5304.

119. Kessler D, Gmachl M, Mantoulidis A, et al. Drugging an undruggable pocket on KRAS. *Proc Natl Acad Sci U S A*. 2019;116(32):15823-15829.

120. Wankhede D, Bontoux C, Grover S, Hofman P. Prognostic Role of KRAS G12C Mutation in Non-Small Cell Lung Cancer: A Systematic Review and Meta-Analysis. *Diagnostics*. 2023;13(19):3043.

121. Margonis GA, Kim Y, Spolverato G, et al. Association Between Specific Mutations in KRAS Codon 12 and Colorectal Liver Metastasis. *JAMA Surg*. 2015;150(8):722-729.

122. Serrano C, Simonetti S, Hernández-Losa J, et al. BRAF V600E and KRAS G12S mutations in peripheral nerve sheath tumours. *Histopathology*. 2013;62(3):499-504.

123. Hobbs GA, Baker NM, Miermont AM, et al. Atypical KRASG12R mutant is impaired in PI3K signaling and macropinocytosis in pancreatic cancer. *Cancer Discov*. 2020;10(1):104-123.

124. Hofmann MH, Gerlach D, Misale S, Petronczki M, Kraut N. Expanding the Reach of Precision Oncology by Drugging All KRAS Mutants. *Cancer Discov*. 2022;12(4):924-937.

125. Fiala O, Buchler T, Mohelnikova-Duchonova B, et al. G12V and G12A KRAS mutations are associated with poor outcome in patients with metastatic colorectal cancer treated with bevacizumab. *Tumor Biology*. 2016;37(5):6823-6830.

126. Bannoura SF, Khan HY, Azmi AS. KRAS G12D targeted therapies for pancreatic cancer: Has the fortress been conquered? *Front Oncol*. 2022;12:1013902.

127. Zhang Z, Guiley KZ, Shokat KM. Chemical acylation of an acquired serine suppresses oncogenic signaling of K-Ras(G12S). *Nat Chem Biol*. 2022;18(11):1177-1183.

128. Zhang Z, Morstein J, Ecker AK, Guiley KZ, Shokat KM. Chemoselective Covalent Modification of K-Ras(G12R) with a Small Molecule Electrophile. *J Am Chem Soc*. 2022;144(35):15916-15921.

129. Duan X, Zhang T, Feng L, et al. A pancreatic cancer organoid platform identifies an inhibitor specific to mutant KRAS. *Cell Stem Cell*. 2024;31(1):71-88.e8.

130. Klochkov SG, Neganova ME, Yarla NS, et al. Implications of farnesyltransferase and its inhibitors as a promising strategy for cancer therapy. *Semin Cancer Biol*. 2019;56:128-134.

131. Baranyi M, Molnár E, Hegedűs L, et al. Farnesyl-transferase inhibitors show synergistic anticancer effects in combination with novel KRAS-G12C inhibitors. *British Journal of Cancer*. 2024;130(6):1059-1072.

132. Kazi A, Xiang S, Yang H, et al. Dual farnesyl and geranylgeranyl transferase inhibitor thwarts mutant KRAS-driven patient-derived pancreatic tumors. *Clinical Cancer Research*. 2019;25(19):5984-5996.

133. Mondal K, Posa MK, Shenoy RP, Roychoudhury S. KRAS Mutation Subtypes and Their Association with Other Driver Mutations in Oncogenic Pathways. *Cells*. 2024;13(14):1221.

134. He Q, Liu Z, Wang J. Targeting KRAS in PDAC: A New Way to Cure It? *Cancers*. 2022;14(20):4982.

135. Dilly J, Hoffman MT, Abbassi L, et al. Mechanisms of resistance to oncogenic KRAS inhibition in pancreatic cancer. *Cancer Discov*. 2024;14(11):2135-2161.

136. Judd J, Karim NA, Khan H, et al. Characterization of KRAS mutation subtypes in non-small cell lung cancer. *Mol Cancer Ther*. 2021;20(12):2577-2584.

137. Sreter KB, Catarata MJ, von Laffert M, Frille A. Resistance to KRAS inhibition in advanced non-small cell lung cancer. *Front Oncol*. 2024;14.

138. Koga T, Suda K, Fujino T, et al. KRAS Secondary Mutations That Confer Acquired Resistance to KRAS G12C Inhibitors, Sotorasib and Adagrasib, and Overcoming Strategies: Insights From In Vitro Experiments. *Journal of Thoracic Oncology*. 2021;16(8):1321-1332.

139. Tanaka N, Lin JJ, Li C, et al. Clinical Acquired Resistance to KRASG12C Inhibition through a Novel KRAS Switch-II Pocket Mutation and Polyclonal Alterations Converging on RAS–MAPK Reactivation. *Cancer Discov*. 2021;11(8):1913-1922.

140. Shaverdashvili K, Burns TF. Advances in the treatment of *KRAS* ^{G12C} mutant non–small cell lung cancer. *Cancer*. 2025;131: e35783.

141. Koga T, Suda K, Fujino T, et al. KRAS Secondary Mutations That Confer Acquired Resistance to KRAS G12C Inhibitors, Sotorasib and Adagrasib, and Overcoming Strategies: Insights From In Vitro Experiments. *Journal of Thoracic Oncology*. 2021;16(8):1321-1332.

142. Dilly J, Hoffman MT, Abbassi L, et al. Mechanisms of resistance to oncogenic KRAS inhibition in pancreatic cancer. *Cancer Discov*. 2024;14(11):2135-2161.

143. Yaeger R, Uboha N V., Pelster MS, et al. Efficacy and Safety of Adagrasib plus Cetuximab in Patients with *KRAS* G12C-Mutated Metastatic Colorectal Cancer. *Cancer Discov*. 2024;14(6):982-993.

144. Liu S V., Nagasaka M, Atz J, Solca F, Müllauer L. Oncogenic gene fusions in cancer: from biology to therapy. *Signal Transduct Target Ther*. 2025;10(1):111.

145. Yuan TL, Amzallag A, Bagni R, et al. Differential Effector Engagement by Oncogenic KRAS. *Cell Rep*. 2018;22(7):1889-1902.

146. Hao MW, Zhang TX, Dong D, Zhou X, Gao H. Enhancing KRAS G12D inhibitor sensitivity in pancreatic cancer through SHP2/PI3K pathway. *Medical Oncology*. 2025;42(5):139.

147. Arbour KC, Jordan E, Kim HR, et al. Effects of Co-occurring Genomic Alterations on Outcomes in Patients with *KRAS* -Mutant Non–Small Cell Lung Cancer. *Clinical Cancer Research*. 2018;24(2):334-340.

148. Skoulidis F, Heymach J V. Co-occurring genomic alterations in non-small-cell lung cancer biology and therapy. *Nat Rev Cancer*. 2019;19(9):495-509.

149. Awad MM, Liu S, Rybkin II, et al. Acquired Resistance to KRAS ^{G12C} Inhibition in Cancer. *New England Journal of Medicine*. 2021;384(25):2382-2393.

150. Isermann T, Sers C, Der CJ, Papke B. KRAS inhibitors: resistance drivers and combinatorial strategies. *Trends Cancer*. 2025;11(2):91-116.

151. Tanaka, N., & Ebi, H. Mechanisms of Resistance to KRAS Inhibitors: Cancer Cells' Strategic Use of Normal Cellular Mechanisms to Adapt. *Cancer Science*. 2025;116(3):600-612.

152. Zhu C, Guan X, Zhang X, et al. Targeting KRAS mutant cancers: from druggable therapy to drug resistance. *Mol Cancer*. 2022;21(1):159.

No primary research results, software or code have been included and no new data were generated or analysed as part of this review.